Inorganic Stereochemistry: Geometric Isomerism in Bis-Tridentate Ligand Complexes

Natalija Pantalon Juraj and Srećko I. Kirin*

Ruđer Bošković Institute, Bijenička 54, HR-10000 Zagreb, Croatia

E-mail: Srecko.Kirin@irb.hr

Abstract

In this review, we analyze the stereochemistry of hexacoordinated metal complexes with flexible tridentate ligands. Unlike rigid ligands, which can adopt only specific coordination modes, flexible ligands open more possibilities to fine-tuning the system for a specific application. Bis-tridentate **[M(A-B-A)$_2$]** complexes of flexible ligands can form three geometric isomers: *mer*, *trans-fac*, and *cis-fac*. The analysis of crystallographic data for 844 structures found in the CSD elucidates influences on the formation of different isomers, such as steric and electronic properties of the ligand and metal ion, type and substitution of donor atoms, and the possibility of non-covalent interactions.

Keywords: stereochemistry; isomer; tridentate ligand; hexacoordinated complex; CSD survey

Graphical Abstract

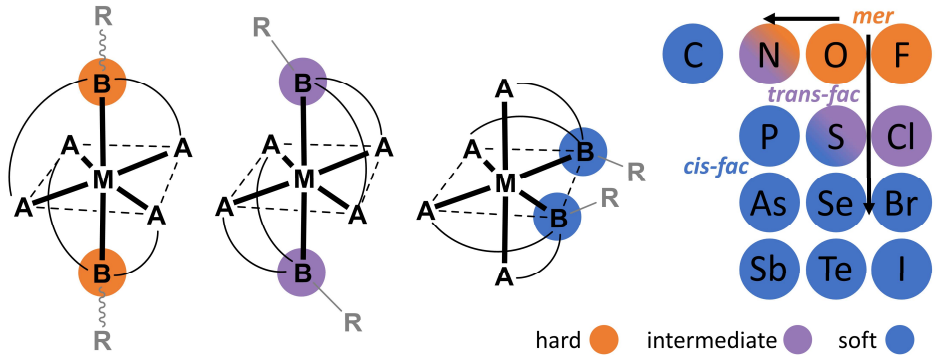

Contents

1. Introduction

The stereochemistry of a given molecule significantly influences a number of important properties like stability and reactivity in a chemical or biological environment. However, the preparation and identification of stereoisomers is often a nontrivial task. In particular, organic stereochemistry is a well-developed discipline, including a number of concepts that foster the application of organic molecules in various fields.[1] On the other hand, different factors governing inorganic stereochemistry are still not well understood.[2,3] The first coordination compounds, mainly Co(III) complexes described by Werner, already intrigued chemists with their stereochemical features. The problem of identifying the isomers of bis-tridentate ligand metal complexes was first encountered in 1934 when the **$[Co(dien)_2]I_3$** complex was isolated by Mann.[4] However, it was not until the 1970s that detailed studies of these isomers were made by Keene and Searle[5,6] as well as Yamasaki and Yoshikawa.[6,7]

Although neglected for an extended period of time due to their saturated coordination sphere, chiral complexes such as **$[Co(en)_3]^{3+}$** (en = ethylenediamine) have found use as efficient hydrogen-bond catalysts,[8] and a number of articles review geometric isomerism in tris-bidentate complexes.[8,9] Bis-tridentate ligand complexes have found use as fluorescent sensors,[10] model compounds for bioinorganic systems,[11] catalysts,[12] and materials with interesting magnetic properties.[13] The most widespread application of **$[M(dien)_2]$** complexes are supramolecular building blocks, where due to the spatial orientation of hydrogen bonds, **$[M(dien)_2]$** act as structure-directing cations in the synthesis of larger inorganic structures.[14] As differences in the stereochemical arrangement lead to different properties of the complexes,[15,16] it is essential to understand these arrangements for specific applications.

The reported studies of **$[M(ligand)_2]$** complex stereochemistry are mainly focused on one or two ligand systems. Favas and Kepert[17,18] described the isomer preferences of bis-tridentate ligand complexes based on repulsion energy calculations; however, clear isomer preferences remain unexplained. Up to date, stereochemical preferences among different ligand systems in bis-tridentate ligand complexes have not been systematically reviewed. Herein, we analyzed crystallographic data of ML_2 structures found in the Cambridge Structural Database (CSD)[19] in order to provide guidelines for the design of these complexes, as well as insight into the coordination behavior of the most commonly used ligands.

2. Dataset

CSD searches (CSD version 5.42, update November 2020) of homoleptic bis-tridentate ligand complexes corresponding to the general structure shown in Figure 1 gave 844 results. In the ML_2 complexes, the central metal atom is saturated by two tridentate A-B-A ligands, containing one central B_{donor} atom with the possibility of a substituent R (tail), and two identical terminal coordination sites (arms) with A_{donor} atoms, forming five-membered chelate rings upon coordination to the metal. According to their symmetry, these ligands can be classified as palindromic.[20] The majority of examples were found for ligand groups shown in Figure 1, while ligands with less than ten reported ML_2 structures are discussed separately (Figure 16). Rigid ligands, such as terpyridine (**terpy**) that only coordinate meridionally and macrocyclic ligands, such as 1,4,7-triazacyclononane (**tacn**) that can only coordinate facially, were not considered.

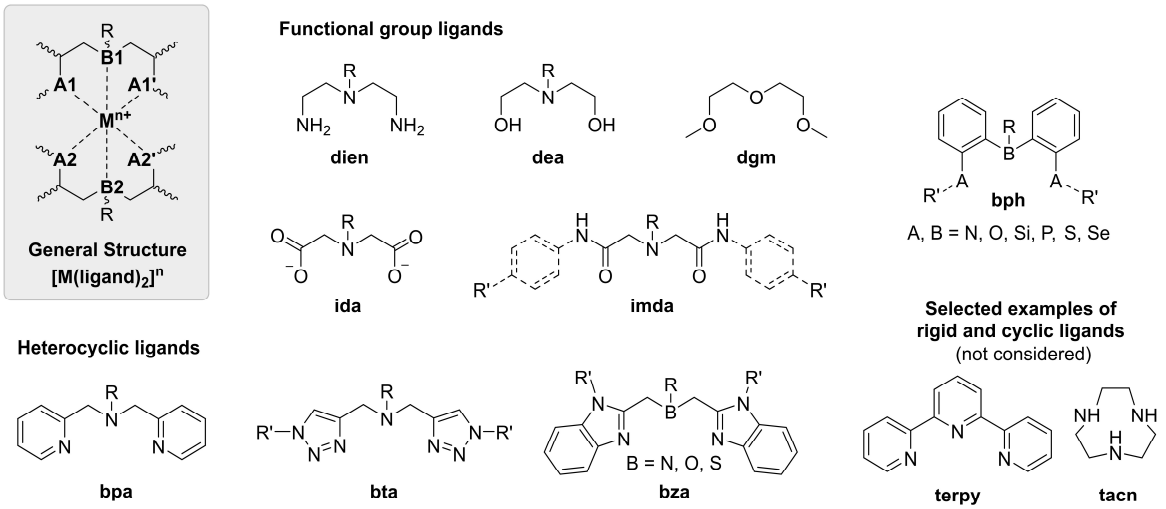

Figure 1. General structure of ML_2 complexes, where B_{donor} = central donor atom, R = substituent on B (tail), and A_{donor} = identical terminal donor sites (arms). Tridentate A-B-A ligands with more than 10 ML_2 structures reported in the CSD. The ligands can have different B_{donor} atoms, which are equally represented in **bph** and **bza** ligands, while only the most common B_{donor} atom is shown for the rest.

In the graphic displays of the structures throughout the review, only the **[M(ligand)$_2$]^n** complex ions are shown, while the counterion and solvent molecules, as well as non-relevant hydrogen atoms present in the crystal structure are omitted unless relevant for the discussion. The structures are identified using their CSD Refcodes. It should be noted that the crystal structure does not necessarily represent the most stable structure. Still, specific trends can be observed from the analysis of crystallographic data[21] and are supported by DFT and solution-state data where available.

3. Isomers of [M(A-B-A)$_2$] complexes

The three geometric isomers of **[M(A-B-A)$_2$]** complexes are *mer*, *trans-fac*, and *cis-fac* (Figure 2), in some publications also denoted as *mer* (meridional), *s-fac* (symmetrical-facial), and *u-fac* (unsymmetrical-facial), respectively.[22] The isomers can be classified according to their A1-M-A1' (A2-M-A2') and B1-M-B2 angles. Values of A1-M-A1' close to 180° show meridional (*mer*) coordination, where the ligand plane bisects the molecule, while values near 90° indicate facial (*fac*) coordination, where one ligand occupies the triangular face of an octahedron.[23] The angle describing the position of the central donor atoms of the two ligands, B1-M-B2, describes *trans* (180°) or *cis* (90°) coordination. Another parameter that can be used to distinguish between isomers is the A1-B1-B2-A1´ dihedral angle,[24] with the following ideal values: *cis-fac* (54.7°), *trans-fac* (90°), *mer* (180°). Throughout this review, we used the former classification method, as the scatter plot of A-M-A' *vs.* B1-M-B2 angles (Figure 3) offers an easy distinction between the isomers as well as information about the geometry. In non-centrosymmetric structures, the A-M-A' angle values slightly differ for the two ligands, and the average of the two A-M-A' angles is used in the analyses.

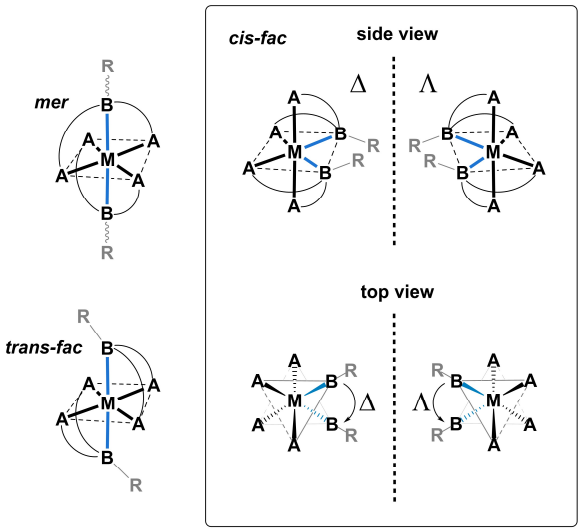

Figure 2. Three geometric isomers of **[M(A-B-A)$_2$]** complexes: *mer*, *trans-fac* and *cis-fac*. The two enantiomers of *cis-fac*, Δ and Λ, are shown from the side view and top view showing the assignation of the chirality descriptor.

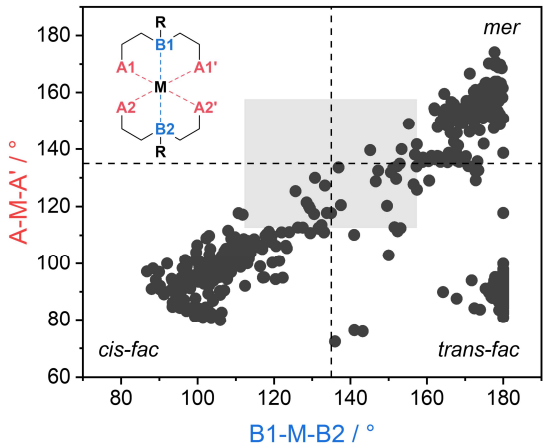

Figure 3. Scatter plot of A-M-A' *vs.* B1-M-B2 angles for 844 analyzed structures. The angle values of 135° indicate borders between isomers; *cis-fac* at the bottom left, *trans-fac* at bottom right, and *mer* at top right. Structures located near the corners of the plot have octahedral geometry, while the middle of the plot indicated by the gray area corresponds to trigonal prismatic geometry.

For the coordination number six, octahedral geometry is more common and characteristic for ionic complexes, while trigonal prismatic geometry is preferred for more covalent metal-ligand combinations such as ligands with soft donor atoms and metals in high oxidation states.[25] Octahedral geometry is characterized by values of A-M-A' and B1-M-B2 angles near 90° or 180°, while values near 135° indicate trigonal prismatic geometry.[18,26] As the octahedral geometry gets more distorted towards trigonal prism, the distinction between different isomers becomes less clear, and in some cases those complexes can be classified differently by different methods. For additional determination of the geometry, we used the program FindGeo,[27] that compares the polyhedron around the metal ion with templates from a library and determines the best match of geometry.

In terms of symmetry, *trans-fac* (C_{2h}) is achiral and can be discriminated from other isomers by its lack of optical properties. The chirality of the *cis-fac* isomer, which has a twofold rotation axis (C_2), arises from the configurational effect; when one ligand coordinates facially, the second ligand has two possible ways of coordination in a *cis-fac* complex, forming either a Δ or Λ enantiomer. The somewhat unexpected chirality of the *mer* isomer (C_2) is a result of the puckered chelate rings and orientation of the substituents on the central B_{donor} atoms. The two conformers of *mer*, δ and λ, were first described for a *mer*-**[Co(dien)$_2$]$^{3+}$** complex,[6,28] where the two N-H bonds on the central donor nitrogen atoms formed a segment of a right- or left-handed helix. This "NH chiral effect" is also valid

for ligands with a substituent R on the central nitrogen atom,[29] as well as for other central donor atoms, where it would refer to the direction of the lone pair of an oxygen or sulfur donor atom. In the studies of optically resolved isomers of **[Co(dien)$_2$]$^{3+}$**[7] and **[Rh(dien)$_2$]$^{3+}$** (WEMLIJ[30]), CD spectra showed significantly larger Δε values for the *cis-fac* than for the *mer* enantiomers. This is not surprising, as the chirality of the *mer* isomer is conformational, while the chirality of *cis-fac* is of configurational origin.

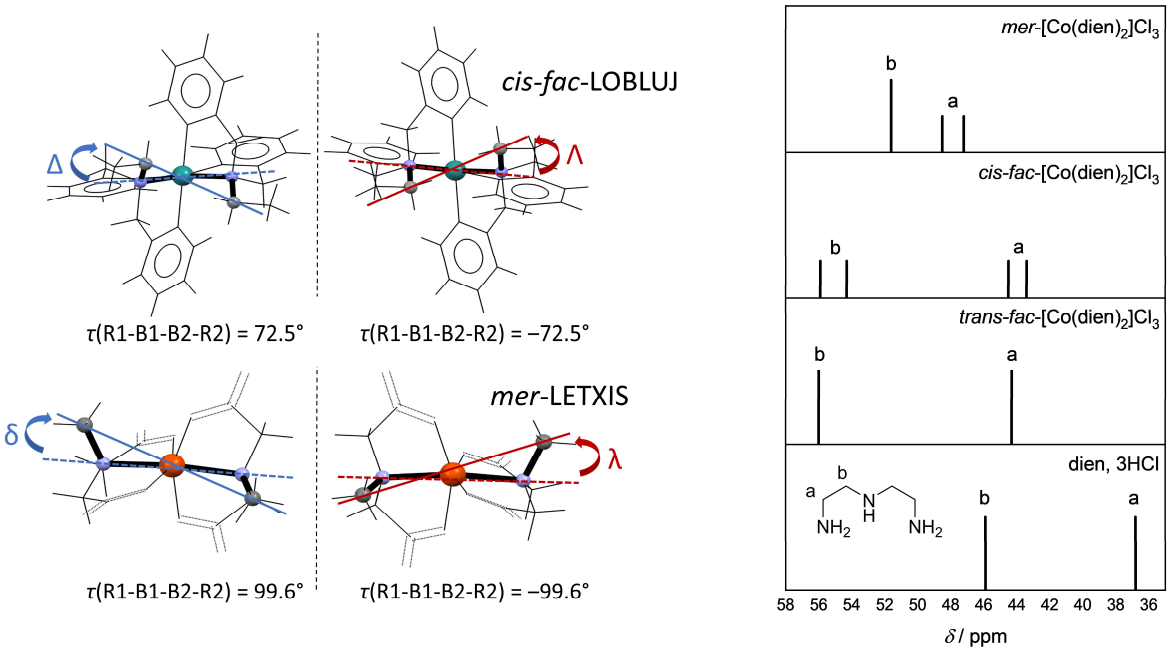

Figure 4. Enantiomers of *cis-fac*-**[Ru(bpa)$_2$]$^{2+}$**, LOBLUJ[31] and *mer*-**[Fe(ida)$_2$]$^-$**, LETXIS[29] (left), both present in the racemic crystal structures. ^{13}C NMR (D_2O) spectra of the free **dien** ligand and three isomers of **[Co(dien)$_2$]Cl$_3$** complexes (right), modified from ref. [32].

The Δ or Λ configurational enantiomers of *cis-fac* and δ and λ conformational enantiomers of *mer* can be assigned according to the helicity of two skew lines. As shown in Figure 4 for structures LOBLUJ and LETXIS, one line connects the two ligating B_{donor} atoms in one plane, and the other connects two R groups above this plane.[33] Numerically, a positive R1-B1-B2-R2 torsion angle corresponds to clockwise rotation (Δ, δ), while a negative torsion corresponds to counterclockwise rotation (Λ, λ). Another way of assigning the *cis-fac* configuration is from the top view of the complex (Figure 2), considering the clockwise (Δ) or counterclockwise (Λ) direction from the top R group (higher priority) towards the bottom R group (lower priority). The Δ and Λ, as well as δ and λ chirality descriptors refer to the chirality of the individual complex cation, while the crystal structure can contain one or both enantiomers. In our dataset, 29% *mer*, 8% *trans-fac*, and 22% *cis-fac* structures were found to crystallize in non-centrosymmetric space groups. The *trans-fac* isomer is expected to be centrosymmetric, and some of the 8% that crystallize in non-centrosymmetric space groups have distorted geometry making their isomer classification somewhat ambiguous. However, a small number of *trans-fac* with regular octahedral geometry also lack a centre of symmetry (for example VOYKOM[34]). Chiral complexes crystallized in centrosymmetric space groups are necessarily racemates, while those in non-centrosymmetric space groups usually contain single enantiomers (conglomerates) but in some cases they can also be racemates.[1] For example, structures of racemates containing both enantiomers as two crystallographically independent complex cations in the unit cell can crystallize in both centrosymmetric (BACDEP[35]) and non-centrosymmetric space groups (TEZBIL[36]). However, the structure TEZBIL contains glide plane symmetry (*n*), a symmetry element that changes the handedness (chirality) of the object. The symmetry of the complex cations

affects the intermolecular interactions and is important to consider in stereospecific interactions among various complex species.[37]

Ligands described in this review form five-membered chelate rings upon coordination to the metal, forming different conformers depending on the chelate ring conformations. Each chelate ring is defined by five torsion angles, and the δ or λ conformation can be assigned for the τ(A-C-C-B) angle of each chelate ring, using the same principle as described for the *mer* isomer. In this case, the bottom line connects two ligating atoms, and the top line connects the two C-C atoms (Figure 5). A situation where A-B is parallel to C-C corresponds to the envelope form with τ(A-C-C-B) = 0.

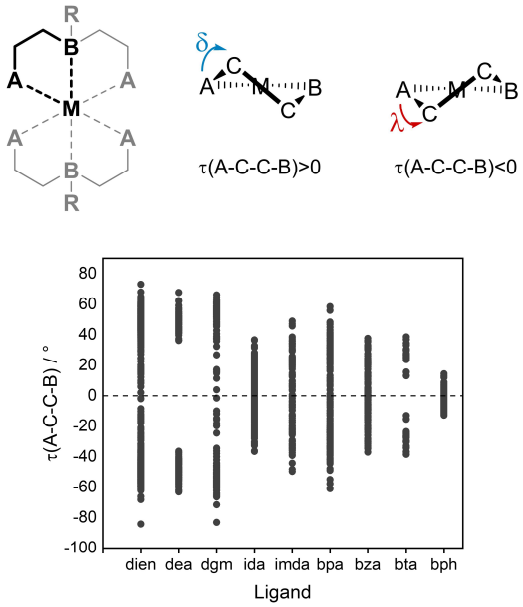

Figure 5. Assigning the conformation of five-membered chelate rings (top) and τ(A-C-C-B) values for the analyzed structures (bottom).

Analysis of the τ(A-C-C-B) torsion angles (Figure 5) rather expectedly shows that flexible **dien** ligands have the widest, while **bph** have the narrowest range of these values, due to the rigid phenyl groups being part of the chelate rings. Small τ(A-C-C-B) values indicate envelope-like conformations of the chelate rings and are not observed for complexes of **dea** and **bta** ligands.

The three isomers can be distinguished in solution by NMR spectroscopy. As described by Searle and Keene,[32] for **[Co(dien)$_2$]Cl$_3$** complexes, ^{1}H NMR was only moderately useful, as difficulties in understanding the splitting patterns of the NH_2 group did not allow unambiguous assignation of the isomer. This was possibly due to the dependence of the splitting pattern on ring conformational interchanges or interactions of the NH_2 groups with anions. On the other hand, ^{13}C NMR spectra gave a clear distinction between the isomers (Figure 4). The number of peaks is related to the point group symmetry; in the C_{2h} *trans-fac* complex, all four a- and all four b-carbon atoms are equivalent, each showing one peak in the ^{13}C spectrum. In the C_2 *cis-fac*, two equatorial and two axial groups give in total four signals. In the *mer* isomer, four signals would be expected for the C_2 point group; however, *mer*-**[Co(dien)$_2$]Cl$_3$** showed three peaks in the intensity ratio of 2:1:1. The magnetic non-equivalence of two carbon atoms was explained as a consequence of non-covalent interactions of neighboring NH_2 groups, influencing the carbon atoms adjacent to the NH_2 groups, while the carbon atoms bound to the secondary amine groups were in similar stereochemical environments and remained magnetically equivalent. For other ligand systems, information about the solution structure could also be obtained by ^{1}H NMR, see Chapter 4.5.

The scatter plot of A-M-A' *vs.* B1-M-B2 angles for all 844 analyzed structures, Figure 3, shows that *trans-fac* complexes are mainly concentrated around values typical for octahedral geometry (90° or 180°), while *mer* and *cis-fac* are more dispersed towards trigonal prismatic geometry (135°). Deviations of the A-M-A' and B1-M-B2 angles from ideal octahedral geometry were described using

mean absolute error (MAE) values, calculated as: $MAE = \frac{1}{n}\sum_{i=1}^{n}|\angle_i - \angle_{ideal}|$, and are shown in Table 1. For the 844 **[M(A-B-A)$_2$]** complexes, larger deviations are observed for the B1-M-B2 angle in *cis-fac* and the A-M-A' angle in *mer*.[7,38,39] To show that the deviations are characteristic for different isomers, regardless of the type of metal or ligand, the same analysis was made for 125 **[Ni(dien)$_2$]$^{2+}$** complexes. The analysis of **[Ni(dien)$_2$]$^{2+}$** complexes (Table 1) showed similar trends as the general analysis, despite the preference of Ni(II) for octahedral geometry and minimal steric requirements of **dien** ligands.

Table 1. Deviations (MAE) of B1-M-B2 and A-M-A' values from ideal octahedral geometry for all analyzed 844 **[M(A-B-A)$_2$]** and for 125 **[Ni(dien)$_2$]$^{2+}$** complexes, shown as ideal octahedral value and (MAE).

	[M(A-B-A)$_2$]		**[Ni(dien)$_2$]$^{2+}$**	
Isomer	**B1-M-B2 /°**	**A-M-A' /°**	**B1-M-B2 /°**	**A-M-A' /°**
mer	180 (7.51)	180 (**25.38**)	180 (2.96)	180 (**17.77**)
trans-fac	180 (2.11)	90 (4.24)	180 (0.54)	90 (1.29)
cis-fac	90 (**16.55**)	90 (10.02)	90 (**12.60**)	90 (5.53)

In *cis-fac* isomers, the B1-M-B2 angle is often larger than 90°, possibly due to steric repulsion of the substituents on the neighboring B_{donor} atoms, leading to distortion towards trigonal prismatic geometry.[17] The deviation of the A-M-A' angle in *mer* describes distortion of the equatorial plane due to the restricted ligand bite angles.[40] In *trans-fac* isomers, the equatorial plane is often tilted; however, the four A_{donor} atoms are predominantly bound in the same plane (Figure 6).

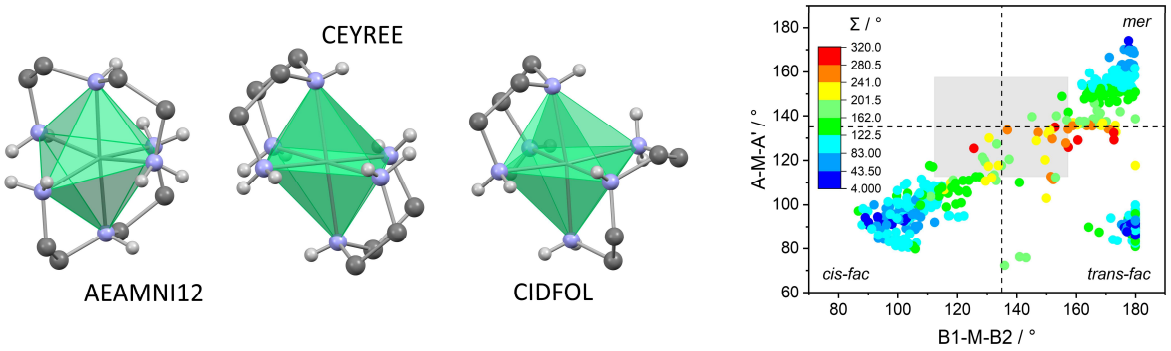

Figure 6. Characteristic examples of coordination polyhedra in *mer*-AEAMNI12,[41] *trans-fac*-CEYREE,[42] and *cis-fac*-CIDFOL[42] isomers of **[Ni(dien)$_2$]$^{2+}$** complexes. Scatter plot of A-M-A' *vs.* B1-M-B2 angles showing values of parameter Σ for all 844 analyzed **[M(A-B-A)$_2$]** structures.

Several different parameters can be used to describe the geometry of hexacoordinated complexes.[43,44] The description of distortion of B1-M-B2 and A-M-A' angles from ideal octahedral values is useful specifically for this system, as it shows the origins of distortion. A more general parameter, the distortion parameter Σ, describes the sum of deviations of 12 *cis* A/B_{donor}-M-A/B_{donor} angles from 90° of an ideal octahedron (Figure 6). Σ = 0 denotes an ideal octahedron, and its values increase with deformation. This parameter is often used for spin-crossover complexes, as differences in the spin state are reflected in different distortions, the Σ parameter often being smaller for low-spin complexes.[13,45,46] A similar way of describing distortion are the bond-angle variance σ^2_{oct} and quadratic elongation λ_{oct}. These parameters are often used for describing structural strain in minerals.[47,48]

4. Ligands

4.1. Diethylenetriamine (dien) ligands

[M(dien)$_2$] complexes are frequently used as complex cations in larger structures such as clusters,[49,50] heterometallic complexes,[51] and chiral frameworks.[52] Using metal complexes instead of organic cations as structure-directing species offers integration of the interesting electronic, magnetic, and optical properties of the metal complexes into the inorganic structures. The preparation of these inorganic structures, such as chalcogenidometalates (Figure 7) with **[M(dien)$_2$]** as structure-directing cations,[14,53] shows the importance of understanding the isomer preferences, as the selected isomer can influence the overall structure.[54]

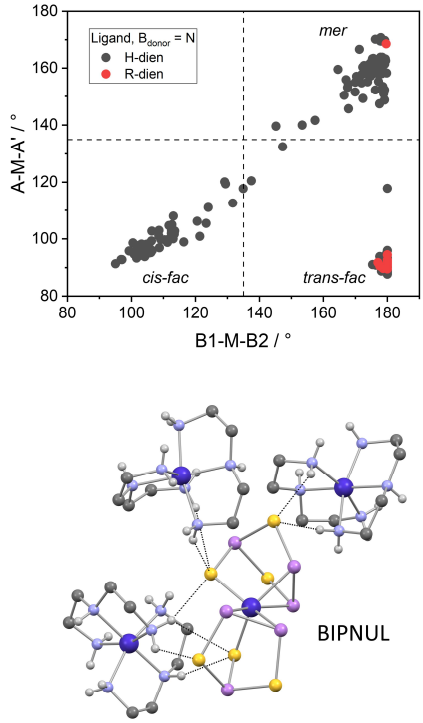

Figure 7. Scatter plot of A-M-A' *vs.* B1-M-B2 angles for 295 **[M(dien)$_2$]** complexes prepared with **H-dien** and **R-dien** ligands with B$_{donor}$ = N. An example of **[M(dien)$_2$]** complexes as structure-directing cations in a thioarsenate structure **[Co(dien)$_2$][Co(As$_3$S$_3$)$_2$]** (BIPNUL).[14]

The similarity of donor atoms and lack of steric hindrance in **dien** ligands already imply a small energy difference between the isomers. For the 295 **[M(dien)$_2$]** complexes, a significant number of all three isomers were found, Figure 7. In the most common case, when the central donor atom B$_{donor}$ = N, there is a possibility of a third substituent (tail); H or R. Dividing the ligands according to the H/R group shows that **H-dien** ligands equally form all three isomers, while the 18 **R-dien** complexes are found almost exclusively as *trans-fac* (Figure 7). The only example of a *mer*-**[M(R-dien)$_2$]** complex is UFEQOL. *Mer*-UFEQOL and *trans-fac*-UFEQUR[55] both have R = Me and are prepared with different counterions, Br^-/PF_6^- and SO_4^{2-}, respectively, which could be a possible cause of the formation of different isomers. Many studies were performed on **H-dien** complexes with the inert Co(III) ion, which lead to the isolation of all three isomers from the mixture. For example, Yamasaki and Yoshikawa reported the isomer ratio of *trans-fac* : *cis-fac* : *mer* = 7 : 30 : 63.[7] Gutiérrez-Zorrilla and coworkers [24] analyzed geometrical parameters of **[M(H-dien)$_2$]** complexes and compared them to their experimentally obtained *trans-fac* and *mer*-**[Ni(H-dien)$_2$]$^{2+}$** complexes (HOKXAG, HOKXEK). DFT calculations of isolated molecules in the gas phase showed that the *mer* isomer was the most stable by 18.8 kJ mol^{-1}. Electrochemical studies of **[Co^{III}(H-dien)$_2$]$^{3+}$** and **[Co^{II}(H-dien)$_2$]$^{2+}$** complexes showed that for the kinetically labile Co(II) ion, only the thermodynamically favored *mer* isomer could be observed. For a **dien** ligand methylated at the B$_{donor}$ atom, the isomer preferences were significantly shifted to *trans-fac*, which was the only isomer observed both in **[Co^{III}(Me-dien)$_2$]$^{3+}$** and **[Co^{II}(Me-dien)$_2$]$^{2+}$**.[56] The H atom on the central donor atom of the ligand results in substantially different properties of the ML$_2$ complexes compared to other possible R groups. Therefore, the more

predictable preference found for the R-ligand can be considered the standard preference of the ligand type. The influence of the R/H group will be described in detail later, see Chapter 5.2.

4.2. Diethanolamine (dea) ligands

The different electronic properties of A_{donor} and B_{donor} atoms in **dea** suggest larger energy differences between isomers than observed for **dien** ligands. For **[M(dea)$_2$]** complexes, the preference of 38 **R-dea** complexes in the solid-state was exclusively *trans-fac*, while one *mer*, one *cis-fac*, and seven *trans-fac* isomers were found for **H-dea** ligands. Yamaguchi and Sakiyama studied the relative stability of **[Ni(H-dea)$_2$]$^{2+}$** isomers based on electronic spectra and DFT calculations, which showed that *cis-fac* was the most stable.[57] A compound containing two **[Cu(dea)$_2$]$^{2+}$** cations (YILNIT[58]) and a pyromellitic anion showed activity as a homogeneous catalyst for the mild oxidative functionalization of cycloalkanes.

In several complexes, the **dea** ligands are deprotonated, and the number of deprotonated hydroxyl groups can affect the isomer preferences (Figure 8). Complexes with one deprotonated OH are all *cis-fac*, while all with two or three deprotonated OH are *trans-fac* isomers. In the case of four deprotonated OH, several Ti(IV) complexes are *cis-fac*, while one Cu(II) complex (ZAZGEP[59]) is *trans-fac*.

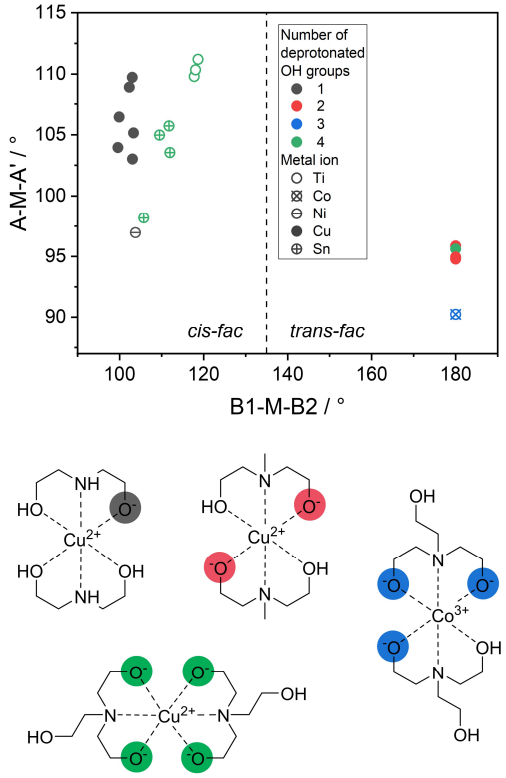

Figure 8. Scatter plot of A-M-A' *vs.* B1-M-B2 angles for 20 **[M(dea)$_2$]** complexes with deprotonated **dea** ligands. A 2D representation of complexes XUCVEX[60], SAGJUG[61], SANHUL,[62] and ZAZGEP[59] with 1, 2, 3, and 4 deprotonated hydroxyl groups of **dea** ligands, respectively.

4.3. Diglycol methyl ether (diglyme, dgm) ligands

Clefts for alkali and alkaline earth metals, such as cyclic polyethers, cryptands, and coordinating solvents, are used to encapsulate cations in systems where only the behavior of the anion is relevant.[63,64] One such cleft is diglyme (**dgm**), an organic solvent often found to coordinate alkali metals forming **[M(dgm)$_2$]** complexes. These complexes are found as part of electrolytes, for example,

in rechargeable magnesium batteries.[65,66] Due to their ionic nature, the **[Li(dgm)$_2$]$^+$** complexes are all *mer* isomers, while **[Na(dgm)$_2$]$^+$** are borderline *mer* or *trans-fac*, with A-M-A angle values around 135° (Figure 9), indicating distortion of the octahedral equatorial plane, characteristic for *mer* complexes.

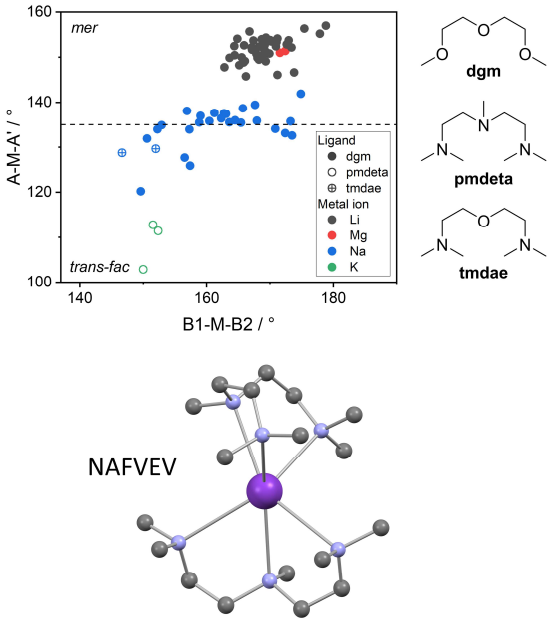

Figure 9. Scatter plot of A-M-A' *vs.* B1-M-B2 angles for 74 **[M(dgm)$_2$]** complexes for ligands **dgm**, **pmdeta**, and **tmdae**. Distorted coordination geometry of a **[K(pmdeta)$_2$]$^+$** complex NAFVEV.[67]

The bite angle, in the case of tridentate ligands the A-M-B angle, is a parameter often used in describing bidentate ligands and is important in catalysis as it affects the rate and selectivity of reactions catalyzed by metal complexes.[68] Mirzaei and coworkers[69] described how the N-M distances and N-M-N angles in five-membered chelate rings formed by coordination of bidentate N-N ligands change to fit the requirements of different metal ions. Namely, as the metal ion size increases, the N-M-N angle becomes smaller while the corresponding M-N bond becomes longer. Kepert defined the normalized bite, b, that describes the contribution of both the metal-ligand distance and ligand bite.[17,18,70] In the case of **[M(A-B-A)$_2$]** complexes, b would be defined as b = 2sin(A-M-B/2). Figure 9 shows the dependence of geometrical parameters on the type of metal. Namely, the A-M-A angle values follow the trend $Li^+ \approx Mg^{2+} > Na^+ > K^+$, inversely proportional to the metal ion size. This can be correlated with the bite angle and normalized bite; for larger metal cations, the A/B$_{donor}$-M distances become longer, the bite angle (A-M-B) and normalized bite, and consequently the A-M-A angle become smaller. Consequently, increasing the metal cation size leads to distortion in the coordination geometry of *mer* complexes (Figure 9).

Due to their similar coordination behavior, a few examples of N,N,N',N",N"-pentamethyldiethylenetriamine (**pmdeta**) and N,N,N',N'-tetramethyldiaminoethyl ether (**tmdae**) complexes were analyzed together with **dgm** ligands. Changing the terminal A$_{donor}$ atoms from O to N gives a ligand with an additional methyl substituent that is more sterically demanding than the **dgm** ligand. These steric properties influence the coordination behavior of the ligands, making it harder to obtain ML$_2$ stoichiometry for **pmdeta** than **dgm**, and often leading to formation of ML complexes with **pmdeta**.[71,72]

4.4. Iminodiacetate (ida) ligands

Inspired by the well-known metal chelator EDTA, the chelator iminodiacetic acid, predominantly in its deprotonated form, iminodiacetate, is a ligand widely used in aqueous environments.[73] **R-ida** ligands predominantly form *trans-fac*, while both *cis-* and *trans-fac* are found for **H-ida** complexes. For the only *mer* complex **[Fe(Me-ida)$_2$]$^-$** (LETXIS[29]), the authors showed that the *mer* configuration was retained in solution. Additionally, using DFT calculations, the authors showed that *mer* was the most stable isomer due to higher repulsive interactions in the ligand framework of *cis-fac*, and the weakest metal-ligand interactions and highest ligand strain in the *trans-fac* isomer. These results are somewhat surprising, as the majority of other **R-ida** complexes were found as *trans-fac*, which in this case was by far the least stable isomer. The reason for this could perhaps be the small size of the R = methyl group, which has in several cases lead to less predictable isomer preferences (see

Table 2).

The non-coordinated carbonyl groups of **ida** ligands offer the possibility of formation of supramolecular structures. **[M(ida)$_2$]** can interact with s-block metal cations such as K^+, Na^+, Cs^+, Ba^{2+}, and Ca^{2+} that are present in the structure for charge neutralization. It is apparent that **ida** ligands generally have *trans-fac* preferences, but interactions of their carbonyl groups with cations render the preferences unpredictable (Figure 10). Generally, **ida** ligands appear to prefer *fac* coordination over *mer*. The two oxygen atoms available for further coordination enable ida ligands to form structures with extended metal-oxygen-metal connectivity, with the possibility of forming porous materials with properties similar to aluminosilicates.[74] A structure of a 3D MOF, **{[Cu$_3$Yb$_2$(ida)$_6$]·8H$_2$O}$_n$**, consists of **[Cu(ida)$_2$]$^{2-}$** units (NOPDUU[75]), where the four non-coordinated oxygen atoms bind to Yb(III) ions, forming a 3D structure (Figure 10). Such MOF-s catalyzed the aerobic oxidation of cycloalkenes.

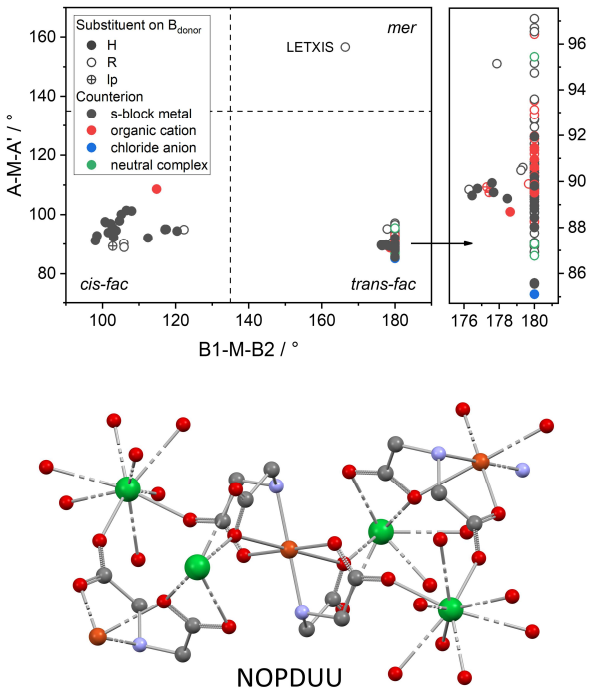

Figure 10. Scatter plot of A-M-A' *vs.* B1-M-B2 angles showing the presence of s-block metals in the structures of 133 **[M(ida)$_2$]** complexes. Interaction of **ida** carbonyl groups with Yb^{3+} cations in a 3D MOF structure NOPDUU.

In the preparation of **ida** complexes, the pH is often adjusted with the addition of a base, and complexes are formed with deprotonated **ida** ligands. However, in five reported **ida** complexes, one or both hydroxyl groups of the ligand were protonated, causing the preferable coordination of the carbonyl oxygen. All five examples of protonated **ida** complexes are *trans-fac* Cu(II) complexes. The complexes have elongated octahedral geometry; for example, **[Cu(Hida)$_2$]** WALLUT[76] has elongated

bonds towards the carbonyl groups, while **[Cu(H$_2$ida)$_2$]$^{2+}$** DOJRUS[77] has elongated bonds towards the protonated OH groups and is the only example where a protonated hydroxyl group is coordinated.

4.5. Iminodiacetamide (imda) ligands

ML$_2$ complexes of **imda** ligands are still not thoroughly researched; the literature describing **[M(imda)$_2$]** complexes is focused mainly on their solid-state structure and stereochemistry. **Imda** ligands preferentially form *trans-fac* isomers (Figure 11). In the only two reported *cis-fac* isomers, the ligands have R = H on the central B$_{donor}$ nitrogen and are additionally stabilized by hydrogen bonding of the central amine hydrogen to the counterion; ClO_4^- in **[Ni(H-imda)$_2$]$^{2+}$** IDACNI[78] and SiF_6^{2-} in **[Zn(H-imda)$_2$]$^{2+}$** VOYKUS[34] (Figure 11). For **[Co(R-imda)$_2$]$^{2+}$**, where R is methyl, ethyl, *n*- or *iso*-propyl, *n*-, *iso*- or *tert*-butyl, DFT calculations showed greater stability of *trans-fac* compared to *cis-fac* for Co(II) and Ni(II) complexes of the **R-imda** ligands, in agreement with the experimentally obtained structures. Substitution of the B$_{donor}$ atom increased the energy difference between *trans*- and *cis-fac* compared to **H-imda** complexes.[79] DFT calculations for Cu(II) complexes of **imda** ligands with R = methyl, ethyl, propyl, and butyl, in agreement with the experimental structures, gave *trans-fac* as the most stable and *mer* as the least stable isomer for all four ligands.[80]

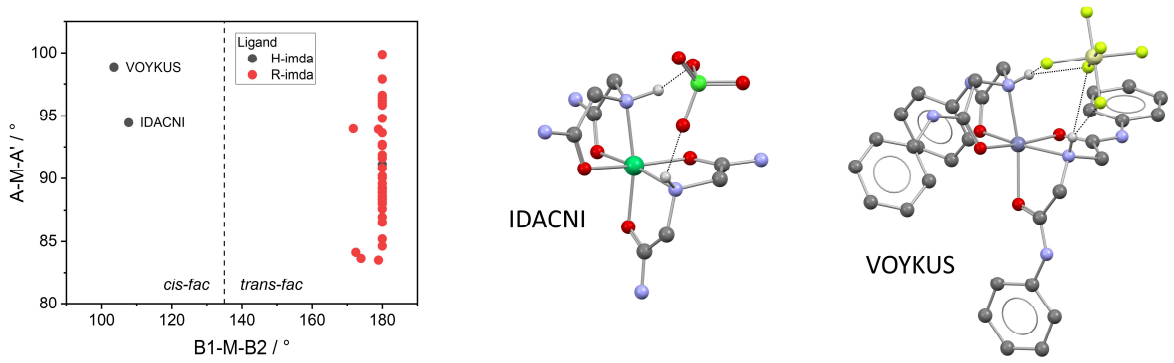

Figure 11. Scatter plot of A-M-A' *vs.* B1-M-B2 angles for 41 **[M(imda)$_2$]** complexes. Stabilization of *cis-fac* isomers by hydrogen bonding to anions in IDACNI[78] and VOYKUS.[34]

In our recent study of **imda** ligands with phenyl-substituted amide groups, electron-donating or withdrawing groups introduced in the *para* position of the phenyl rings enabled fine-tuning of the stereochemical preferences of ML$_2$ complexes.[34] DFT calculations showed that electron-donating groups stabilize the *mer* isomer, while electron-withdrawing substituents promote the stability of *trans-fac*. Upon further addition of substituents, the electronic effects became less evident due to increased steric crowding. The *trans-fac* configurations of complexes with isopropyl-substituted **imda** ligands observed in the crystal structure were also confirmed in solution by ^{1}H NMR spectroscopy. In the free ligand, the equivalent CH$_2$ protons show a single peak. When the ligand is coordinated, two doublets with geminal coupling for the CH$_2$ protons indicate a centrosymmetric structure, i.e., a *trans-fac* isomer.

4.6. Bis(2-pyridylmethyl)amine (bpa) ligands

Bpa ligands are analogs of the well-known metal chelator TPEN and its quinoline derivative TQEN, which have a high affinity for many transition metals and are used as fluorescent probes for detection of Zn(II).[81] For ML$_2$ complexes of **bpa** ligands, 75 structures are reported: 4 *mer*, 21 *trans-fac*, and 50 *cis-fac* isomers. Three *mer*, QUVPED[82] and YOYNIK[83] with two independent complex cations, are Fe(II) complexes with a deprotonated central nitrogen atom of the **H-bpa** ligand (**bpa**$^-$), indicating that ligands with deprotonated central donor nitrogen atoms have a tendency for meridional coordination. **R-bpa** complexes are all *cis-fac*, except for *trans-fac*-BELNOX[84] that is a

Hg(II) complex with trigonal prismatic geometry. Due to the stereochemical diversity of ligands with R = H on the central donor atom, **[M(H-bpa)$_2$]** complexes are found as all three isomers, and their isomer preferences can roughly be correlated to the coordinating ability of the anion (Figure 12). For **[M(H-bpa)$_2$]**, when strongly coordinating anions were used in the synthesis, mainly *trans-fac* isomers and one *mer* (**[Cd(H-bpa)$_2$]$^{2+}$**, ZAYPEW[85]) were found. With weakly coordinating anions, *cis-fac* was the preferred isomer.

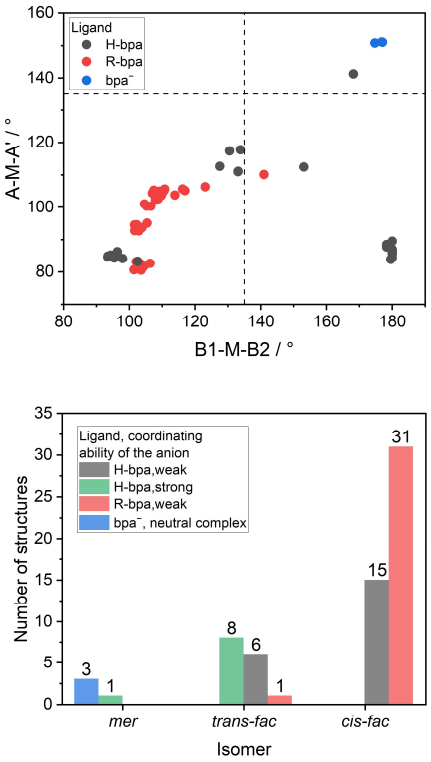

Figure 12. Scatter plot of A-M-A' *vs.* B1-M-B2 angles (top) and distribution of isomers (bottom) for 65 **[M(bpa)$_2$]** complexes with different **H-/R-bpa/bpa$^-$** (B_{donor} = N) ligands and coordinating ability of anions. The anions are classified as strongly or weakly coordinating according to their a^{TM} value.[86]

The counterion could influence the isomer preferences during synthesis, by influencing the reaction mechanism of the ML_2 complex formation, or during crystallization, by stabilizing an isomer with non-covalent interactions.[85,87] For example, anions such as BF_4^- and ClO_4^-, although weak H-bond acceptors,[88] can participate in multiple H-bonds, stabilizing the *cis-fac* isomer as shown in Figure 11.

Due to the observed trends in **bpa** coordination properties for complexes with different anions, we have taken a particular interest in the anion influence in our studies of **[M(bpa)$_2$]** complexes. Depending on the metal salt precursors, we obtained a wide variety of different structures. Firstly, amino acid or amine substituted **bpa** ligands,[89] H-βAla-OMe and H-Gly-OMe derivatives formed Zn(II) coordination polymers due to cleavage of the ester group. Shorter reaction time and changing the anion from nitrate to bromide prevented the ester cleavage and resulted in the formation of ML complexes. Changing the anion to weakly coordinating tetrafluoroborate yielded *cis-fac*-**[M(bpa)$_2$]** complexes, isostructural for Zn(II), Co(II), and Ni(II). ^{1}H and ^{13}C NMR spectra showed that the *cis-fac* isomer of the Zn(II) complex is retained in acetonitrile-d_3 solution. The coordination environment of Zn(II) was studied in detail with DFT calculations, using **Me-bpa** as the model ligand and **Me-dien** and **Me-terpy** for comparison. Comparing the energetics of ML and ML_2 species showed that the bromide anion prevents coordination of the second ligand. In the absence of bromide anions, ML_2 complexes are formed with similar stability of all three isomers and a slight preference for *mer*, both for **Me-bpa** and **Me-dien**. Secondly, we studied the coordination behavior of the ***i*Pr-bpa** ligand.[90] Changing the metal precursor significantly affected the obtained complex structures,

resulting in the formation of ML monomers, bridged dimers, a coordination polymer, a cyclic trimer, and finally, a *cis-fac*-**[Zn(*i*Pr-bpa)$_2$]$^{2+}$** (IHIKAO) complex was obtained with $Zn(ClO_4)_2$. In acetonitrile-d_3 solution, the complex exhibited intermediate ligand exchange compared to the NMR timescale, preventing the determination of the isomer type. However, DFT calculations predicted *cis-fac*-**[Zn(*i*Pr-bpa)$_2$]$^{2+}$** as the most stable isomer, both in vacuum and acetonitrile solution. Llobet and coworkers compared the solid-state and solution structure of a **[Ru(bpa)$_2$]$^{2+}$** complex (LOBLUJ[31]). The crystal structure contained a racemic mixture of Δ and Λ enantiomers of the *cis-fac* isomer. The *cis-fac* configuration was retained in solution, as confirmed by ^{1}H NMR; resonances for two distinct pyridyl rings indicated a structure of C_2 symmetry, and the aliphatic-aromatic inter-ligand NOE effect supported the *cis-fac*, rather than the *mer* configuration.

4.7. Bis-benzimidazole (bza) ligands

Imidazoles and benzimidazoles are extensively studied due to their biological activity.[91] ML_2 complexes of tridentate bis-imidazole ligands are surprisingly rare, with only five such structures in the CSD. For **[M(bza)$_2$]** complexes, 36 structures were found, with variations of the central donor atom, B_{donor} = N, O or S. Here it becomes apparent that the central donor atom type has a significant influence on the stereochemistry. All reported ML_2 complexes of **S-bza** ligands are *trans-fac*, **O-bza** formed both *trans-fac* and *mer*, while **N-bza** formed *cis-* and *trans-fac* (Figure 13).

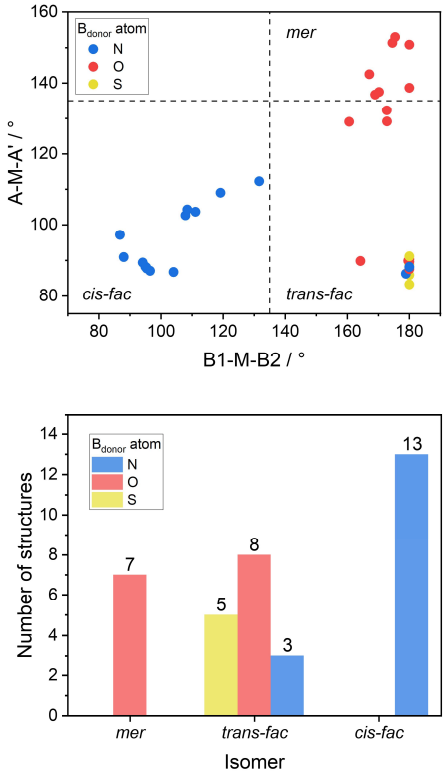

Figure 13. Scatter plot of A-M-A' *vs.* B1-M-B2 angles (top) and distribution of isomers (bottom) for 36 **[M(bza)$_2$]** complexes with different central B_{donor} atoms.

Considering the substituent R on the central B_{donor} = N atom, the standard preference of **R-bza** would be *cis-fac*. **H-bza** complexes are mainly *cis-fac*, except for three *trans-fac* Cu(II) complexes. Interestingly, none of the *cis-fac* complexes was prepared with Cu(II); for a more detailed description of the metal ion influence, see Chapter 5.1.

4.8. Bis-1,2,3-triazole (bta) ligands

Click chemistry offers an easy way of ligand derivatization and incorporation of functional groups into the triazole ligand structure[10] since substituents on the triazole ring can be easily varied. Triazole-for-pyridine substitution described by Sarkar et.al.[92] gives a twist to the extensively studied **bpa** system. With an increasing number of pyridyl arms substituted with triazole in a tripodal tris(pyridylmethyl)amine (TPA) ligand, due to the weaker acceptor properties of triazole compared to pyridine, the increase in electron density at the Ru center lead to weaker coordination of the electron-donating B_{donor} amine nitrogen.

All 12 **[M(bta)$_2$]** complexes found in the CSD are exclusively *trans-fac* isomers, contrary to the observed *cis-fac* preferences of heterocyclic ligands **bpa** and **bza**. The comparison of triazole and pyridine donors gave contradictory results, especially when the rings were part of multidentate ligands, showing that understanding this difference is not trivial.[93] The majority of **bta** complexes found in the CSD are Fe(II) and Co(II) complexes studied by Sarkar and coworkers. They designed tripodal **bta** ligands with different substituents on the triazole rings and studied their effect on the spin-crossover behavior of **[Co(bta)$_2$]$^{2+}$** complexes.[94] The benzyl-substituted ligand gave a complex that acted as a chemical switch, reversibly forming ML and ML_2 complexes by using different metal to ligand ratios, which was accompanied by a high spin to low spin transition. In the ML_2 complex (Figure 14), C-H---π T-stacking interactions influenced the torsion angles at the metal center. These structural changes influenced the ligand field strength and in turn the spin-crossover properties. ML_2 complexes with cyclohexyl substituted ligands, without the possibility of non-covalent interactions in the complex, unlike the benzyl derivative, showed no spin-crossover properties. To further confirm that the spin-crossover behavior was indeed caused by non-covalent interactions rather than just changes in the ligand backbone, they prepared analogous ML_2 Fe(II) complexes with the benzyl-substituted ligand.[13] The presence of solvent molecules in the crystal structure disrupted the stacking interactions and prevented spin-crossover behavior.

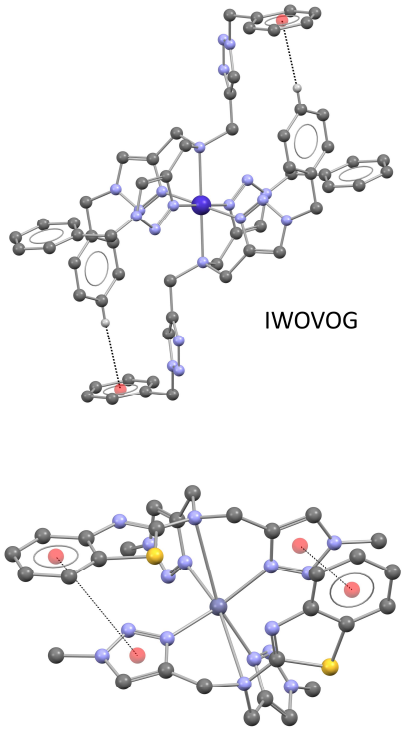

Figure 14. Non-covalent interactions in a **[Co(bta)$_2$]$^{2+}$** complex IWOVOG.[94] An example of π-π interactions in a calculated **[Zn(bta)$_2$]$^{2+}$** complex.[95]

In our recent work,[95] two crystal structures of **[Cu(bta)$_2$]$^{2+}$** complexes had significantly elongated B_{donor}-M distances (2.781 Å and 2.873 Å). As the *trans-fac* isomer, especially for Cu(II), enables elongated B_{donor}-M distances while retaining octahedral geometry, the preference of **bta**

ligands for elongated B_{donor}-M bonds could be a possible cause of their *trans-fac* preference. For Cu(II) complexes, DFT calculations showed *trans-fac*, with significantly elongated B_{donor}-M distances, as the most stable isomer, except for the ligand with R = Me. For Zn(II) complexes, the situation was somewhat different; the smaller methyl and isopropyl groups favor *trans-fac*, the larger phenyl group favors *mer*, and the benzothiazole group favors *cis-fac* due to favorable π-π stacking interactions between the benzothiazole and triazole groups (Figure 14).

4.9. Bisphenyl (bph) ligands

Bisphenyl ligands, unlike the ligands described so far, have rigid phenyl groups in the place of flexible CH_2 linkers connecting the central B_{donor} atom and terminal donor groups. The phenyl rings substituted at the *ortho* position with various donor atoms enable tridentate coordination to transition metals. Despite their rigidness, the geometry around the central B_{donor} atom is flexible enough to allow facial coordination, as long as the B_{donor} atom is not part of a conjugated system. Ligands containing two phenolate donor groups can stabilize high oxidation states due to their π-donating ability.[96] Furthermore, they are often found in the form of phenoxyl radicals used in bioinspired radical catalysis.[97] Chaudhuri and coworkers[96] studied nonoxovanadium(IV) and oxovanadium(V) complexes of **bph** ligands containing soft central donor atoms; S, Se, P, and P=O, finding that these ligands were capable of stabilizing the hexacoordinated nonoxovanadium(IV) moiety without the formation of phenoxyl radical species. With two aromatic rings near the donor atoms, **bph** ligands have the possibility of forming conjugated systems and can act as non-innocent ligands, for example, in HASNEX,[98] ZODKIO, and ZODKUA.[26]

Structures containing **bph** ligands with a variety of central B_{donor} atoms are reported (

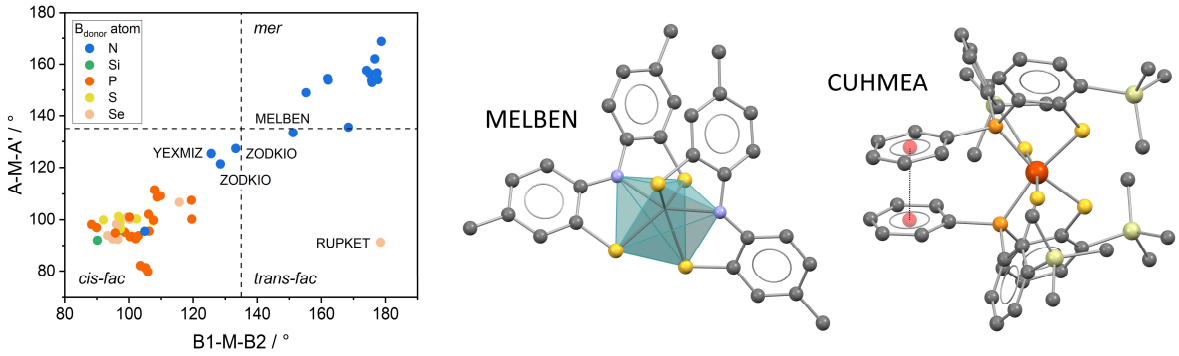

Figure 15). In the case of B_{donor} = N, the central N atom is deprotonated in all complexes except **[Ni(H-bph)$_2$]$^{2+}$** (USIQEU[99]); a *cis-fac* isomer of regular octahedral geometry. When B_{donor} = N is deprotonated, the electron pair can participate in the conjugated system, and the ligand becomes rigid and unable to coordinate facially. A similar possibility was observed in **bpa** ligands, where ligands with a deprotonated central N donor atom formed exclusively *mer* isomers.[83]

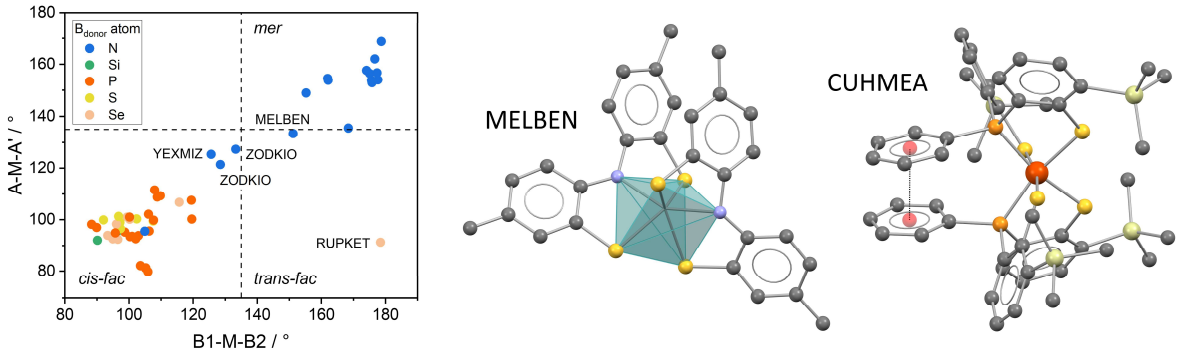

Figure 15. Scatter plot of A-M-A' *vs.* B1-M-B2 angles for 56 **[M(bph)$_2$]** complexes divided according to the B_{donor} atom type. Trigonal prismatic geometry of MELBEN[100] and an example of π-π interactions in a **bph** complex CUHMEA.[101]

On the other hand, three *fac* isomers were found with deprotonated **bph** ligands: *cis-fac* ZODKIO and YEXMIZ,[102] and *trans-fac* MELBEN[100]. While these complexes would formally be classified as borderline *fac* isomers according to their A-M-A' and B1-M-B2 angle values, the large size and trigonal prismatic geometry of the metal cation (Os in ZODKIO, Mo in MELBEN, and Pb in YEXMIZ) enable the ligands to retain the planarity expected for meridional coordination (

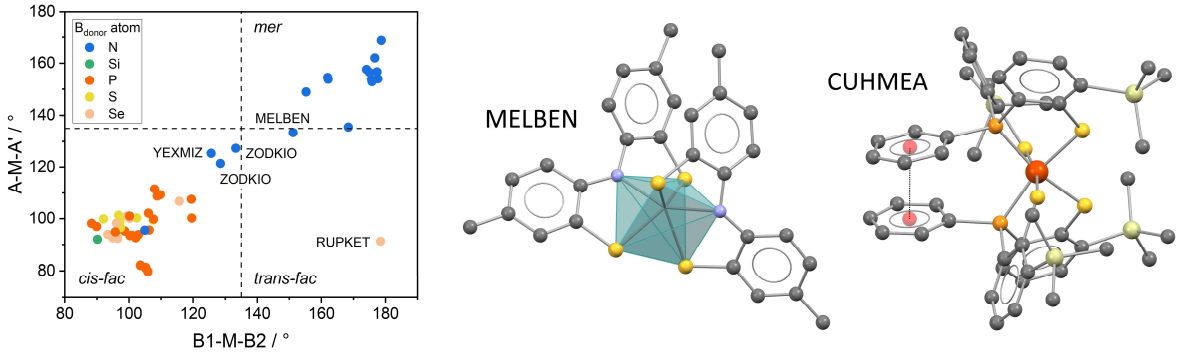

Figure 15). In ligands with B_{donor} = P, the third substituent on the P atom is often an aromatic R group, found in several examples to further stabilize the *cis-fac* isomer with π-π stacking interactions (

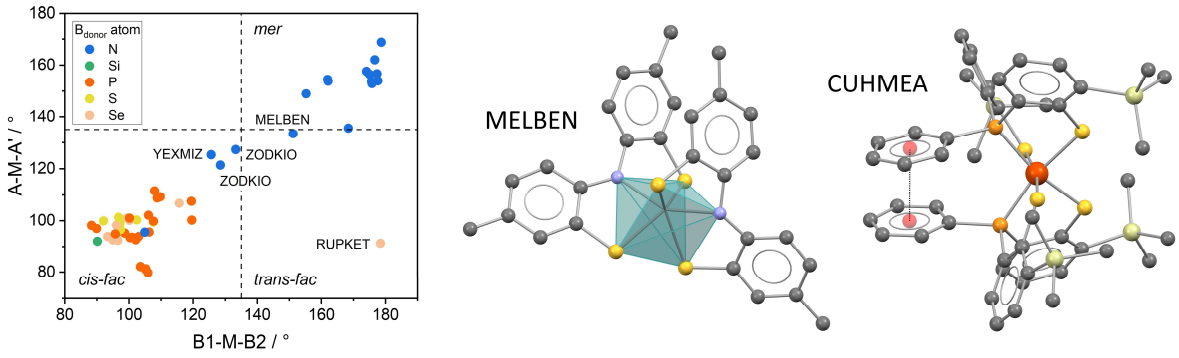

Figure 15).

The only octahedral *trans-fac* has B_{donor} = Se and A_{donor} =O. This particular **[Co(bph)$_2$]$^-$** complex was isolated by Ali et.al. both as a *cis-fac* (RUPKAP) and *trans-fac* (RUPKET) isomer.[103] According to DFT calculations, the authors stated that *trans-fac* was the thermodynamically favored product by 6.7 kcal mol^{-1} due to lessening of the steric repulsion between the bulky *t*Bu groups. However, at lower temperatures, the kinetically favored *cis-fac* isomer was obtained, and additionally stabilized by Van der Waals Se···Se interactions. The phenyl rings of the **bph** ligands can be further substituted at various positions. A common motif is 3,5-disubstitution of the phenyl rings with bulky *tert*-butyl groups. Interestingly, despite the steric bulkiness of these **bph** ligands, the majority of complexes found in CSD were *cis-fac*.

[M(bph)$_2$] complexes are often found with larger second and third-row transition metals, unlike the majority of complexes described so far that contain first-row metals. Brown and Cipressi[26] described octahedral to trigonal prismatic distortion in **bph** complexes of Ru and Os. The somewhat unexpected trigonal prismatic geometry of their Ru and Os complexes compared to other literature examples lead to the conclusion that energetically significant π* interactions are important in understanding the driving force for octahedral to trigonal prismatic distortion.

In an ML_2 complex of an S-P-S **bph** ligand studied by Hsu and coworkers,[104] the bound thiolato group acted as a strong nucleophile, activating dichloromethane, a weak electrophile. Upon the reaction with dichloromethane, two isomeric structures were formed, one with the newly formed thioether group *trans* to the thiolate and the other with the thioether group *trans* to the phosphine donor of the other ligand in the ML_2 complex. A similar complex described by Lee et.al.[101] showed different HNO release from two **bph** complexes where the ligand had either a thiol or thioether group, finding that the thiol group acted as a NO trap due to the intramolecular [SH···ON−Fe] interactions,

leading to release of HNO and formation of a **[Fe(bph)$_2$]** complex (CUHMEA). Lee et.al.[105] studied the oxidation of a Ni(II) complex to Ni(IV). As different oxidation states of Ni prefer different geometries, the ligands used to accommodate a nickel ion upon changes in the oxidation state have to be sufficiently flexible. They started with a square planar Ni(II) complex with two **bph** ligands containing one protonated and non-coordinated thiol group each. Upon oxidation in basic conditions, absorption and EPR spectra showed that the **bph** ligands were deprotonated, forming a hexacoordinated Ni(IV) complex. In the square planar Ni(II) complex, the two ligands are oriented *trans* to each other, but upon oxidation, a *cis-fac* ML_2 complex is formed. The authors used DFT calculations to explain this change in configuration, confirming that the experimentally observed *cis-fac* isomer is indeed the most stable structure.

4.10. Isolated examples

Several types of ligands that correspond to the general search were found with only a few examples of ML_2 complexes in the CSD (Figure 16). In addition to bis-triazole ligands described earlier, ligands containing five-membered heterocyclic rings were found containing imidazole,[40] pyrrole[106], pyrazole,[107] tetrazole,[108] and oxazoline[109] moieties. For example, Ti, Zr, and Hf complexes of pyrrolyl ligands showed analogous C2 symmetric structures of *cis-fac* isomers, and the C2 symmetric structure of the Ti complex was retained in solution.[106]

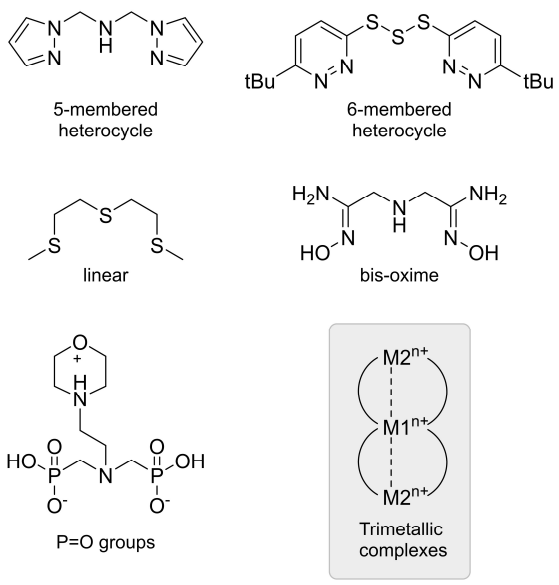

Figure 16. Selected examples of tridentate ligands with <10 examples of ML_2 complexes in the CSD database and general structure of trimetallic complexes.

Braunstein et.al.[109] compared the coordination behavior of **bpa** and bis-oxazoline ligands with phosphorous B_{donor} atoms. Both obtained complexes were *cis-fac* isomers. Addition of methyl substituents to the oxazoline group, increasing the steric requirements, lead to N,N-coordination of the bis-oxazoline ligand and formation of tetracoordinated ML complexes.

Several ligands containing six-membered heterocyclic rings as terminal donor groups were found, with heteroatoms N or S in the place of CH_2 linkers. When comparing complexes WIMNEN and WIMMUC[110] that differ only in the CH_2 / NMe linker, the structures appear to be relatively similar. Tris(pyridylmethyl)phosphine and tris(N-methyl-pyridylamino)phosphine complexes WIMMUC, WIMNAJ, and WIMNEN were prepared as tris(pyridylmethyl)amine (TPA) analogs. Compared to TPA that mainly acts as a tetradentate ligand, the longer M-P bond distance in these ligands compared to the M-N distance in TPA allowed coordination of only two pyridyl groups, forming ML_2 complexes.

A few examples of linear ligands contain various donor atom combinations, such as S-N-S ligands whose ML_2 complexes with Mo and W were used as precursors in chemical vapor deposition

in the synthesis of crystalline MoS_2 and WS_2 thin films with interesting semiconducting and optoelectronic properties.[111] A **[Ni(bis-oxime)$_2$]$^{2+}$** complex (LIYCON[112]) was found to promote dioxygen reactivity in aerobic oxidation of triphenylphosphine. Different phosphorous-containing groups can act as terminal donor sites, such as iminodiphosphonic acid[113] and diphenylphosphine.[114]

Jurkschat et.al.[115] studied the coordination properties of Sn(IV) complexes of amino alcohol ligands. A ligand with an additional CH_2 group, forming six-membered chelate rings, gave a complex of nearly ideal octahedral geometry, while the octahedral geometry in complexes with five-membered chelate rings was severely distorted. The two Sn(IV) complexes with five-membered chelate rings, ZIXZEO and ZIXZOY differ in the substituent on the central B_{donor} atom. ZIXZEO, with R = *n*-butyl, gave a *cis-fac*, while ZIXZOY, with R = *p*-fluorophenyl, formed a *mer* isomer. DFT calculations corresponded to the experimental results; however, for the *p*-fluorophenyl derivative, the energy differences were minimal, indicating that both the *mer* and *cis-fac* isomer could be formed, but only *mer* was observed experimentally.

4.11. Trimetallic complexes

If metals are considered as B_{donor} atoms, 41 structures of trimetallic complexes are found, corresponding to the general structure shown in Figure 16. These complexes are not included in the 844 complexes used in the general analyses. In the literature concerning trimetallic complexes, amidate-hanging Pt mononuclear complexes are often used as precursors, as the non-coordinated O atoms easily bind other metals in the solution.[116,117] The obtained trimetallic complexes can then be used as precursors for the synthesis of one-dimensional chains.[116] In these complexes, central B_{donor} atoms are metals Pt and Au, and the formation of different isomers is often influenced by the *cis* or *trans* configuration of the metal precursor used in the synthesis.

Matsumoto and Chen studied a series of trimetallic complexes prepared with Mn^{2+}, Fe^{3+}, Co^{2+}, Ni^{2+}, Cu^{2+} as central metal atoms, connected to two Pt(II) centers by four amidate ligands.[118] The authors note that the M-Pt distance is considered a consequence of the amidate ligand geometric requirements rather than electronic interaction between the metal centers. However, weak electronic interactions are still possible. The crystal structure of the Mn(II) complex LUJJIJ contains two complex cations of different geometry, where the square planar geometry of Mn(II) in the *trans-fac* complex enabled a shorter Pt-Mn distance than the tetrahedral Mn(II) in the *cis-fac* complex cation (Figure 17).

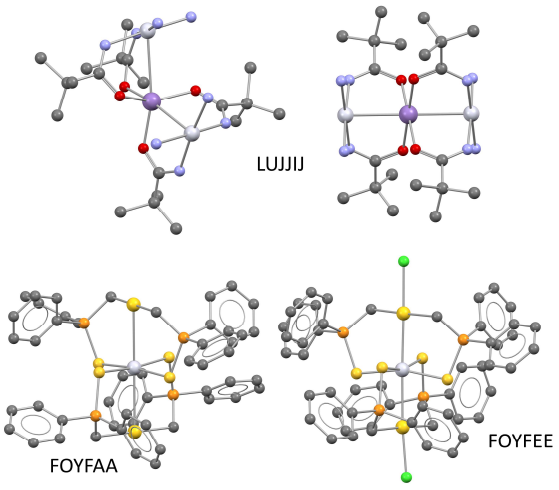

Figure 17. Trimetallic complexes *trans-fac*- and *cis-fac*-LUJJIJ,[118] and *mer*-FOYFAA and *mer*-FOYFEE[119] before and after oxidative halogenation.

Trinuclear ylide complexes were studied in respect to oxidative addition reactions.[119–121] Such three-center, two-electron oxidations of trimetallic complexes lead to partial formation of metal-metal bonds and formation of adducts with halogens or other oxidants. For example, a difference in the Au-Pt distance can be observed in complex FOYFAA and its Cl-adduct FOYFEE (Figure 17).[119]

5. Influences on the stereochemistry

5.1. Influence of the metal cation

The structures of coordination compounds are influenced by different factors, such as valence shell electron pair repulsion (VSEPR) considerations, occupancy of d-orbitals, steric interference, and crystal packing effects, and it is often difficult to determine the relative importance of these factors.[23] ML_2 complexes are found with a variety of metal cations (Figure 18), and the largest number of structures are found with 3d-metals. According to Pearson's hard and soft acids and bases (HSAB) theory,[122] small cations with localized charge, hard acids, preferably bind to hard bases, small donor atoms with localized charge, forming complexes of ionic character. In the same way, soft acids and bases preferably bind to form complexes of covalent character.

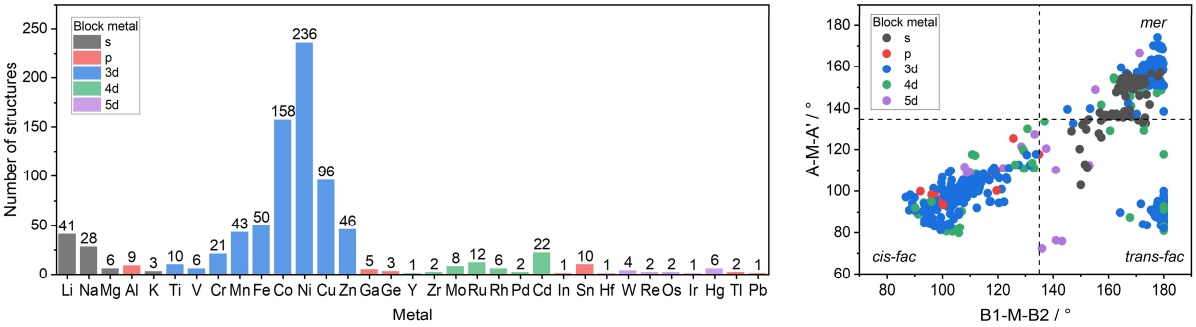

Figure 18. Number of structures found with different metal cations for 844 complexes considered in this study, listed according to the atomic number of the metal (left). Scatter plot of A-M-A' *vs.* B1-M-B2 angles for all 844 **[M(ligand)$_2$]** complexes according to the position of the metal in the periodic table (right).

Examples of ionic complexes discussed herein are s-block metal complexes found with **dgm** ligands (Figure 18). Such complexes mainly adopt meridional coordination or borderline *trans-fac* with distorted geometries. Although ideal octahedral geometry with 90° angles between neighboring donor atoms would be expected for ionic complexes, the bite angle of meridionally coordinated ligands leads to distortion of the equatorial plane with smaller A-M-A' angles. On the other hand, 4d and 5d metals can mostly be classified as soft acids, often forming complexes of trigonal prismatic geometry. Although all three isomers are found for these complexes, *cis-fac* appears to be the prevailing type (Figure 18).

The largest number of structures is found with 3d metals (Figure 18), and Co and Ni complexes are by far the most extensively studied. All three isomers were found for Co and Ni, and their geometries are mainly near octahedral. For kinetically inert complexes, such as **[Co(dien)$_2$]$^{3+}$**, mixtures of all three isomers can be separated by ion-exchange chromatography, while for labile complexes of Co(II), usually only the thermodynamic product can be obtained due to fast isomerization of the complexes.[56] The inert Co(III) complexes are often prepared by oxidation of labile Co(II), obtaining an equilibrium mixture of isomers that can be separated.[28,123,124] For 3d metals other than Co and Ni, generally octahedral geometry is more common, with the exception of Mn(II) complexes that show a wide range of geometrical parameters. For Zn(II) with filled d-orbitals, the coordination is expectedly more dependant on steric than electronic factors.

The specific steric requirements of the Jahn-Teller distortion can influence the stereochemistry of Cu(II) complexes.[125,126] The majority of **[Cu(ligand)$_2$]** complexes are *trans-fac* isomers with octahedral geometry. By comparing bond lengths around the metal center in Cu(II)

complexes (Figure 19), it appears that **bta** and **bza** ligands prefer elongated B_{donor}-M bonds. A more general display of bond lengths in all analyzed complexes with B_{donor} = N ligands (Figure 19) additionally shows that elongation of B_{donor}-M bonds compared to A_{donor}-M bonds is an inherent property of **bta** and **bza** ligands. These structural features could elucidate the particular isomer preferences observed for **bta** and **bza** ligands. In particular, for **N-bza** and **O-bza** ligands, Cu(II) complexes were found to deviate from the isomer preference observed for other metals (Figure 19). This could be rationalized by the fact that in Cu(II) complexes, their Jahn-Teller deformation enables elongated B_{donor}-Cu bonds when the B_{donor} atoms are located *trans* to each other, thus favoring *trans-fac* isomers.[126–128] Two bonds in the *cis* position could also undergo Jahn-Teller elongation; however, that is observed in complexes where the ligand dictates trigonal prismatic geometry, while in octahedral complexes, the Jahn-Teller deformation affects the *trans* bonds.[129] **O-bza** ligands formed both *trans-fac* and *mer* isomers. For Cu(II), *trans-fac* is possibly preferred over *mer*, as *trans-fac* is better suited for octahedral geometry expected for Cu(II) complexes.

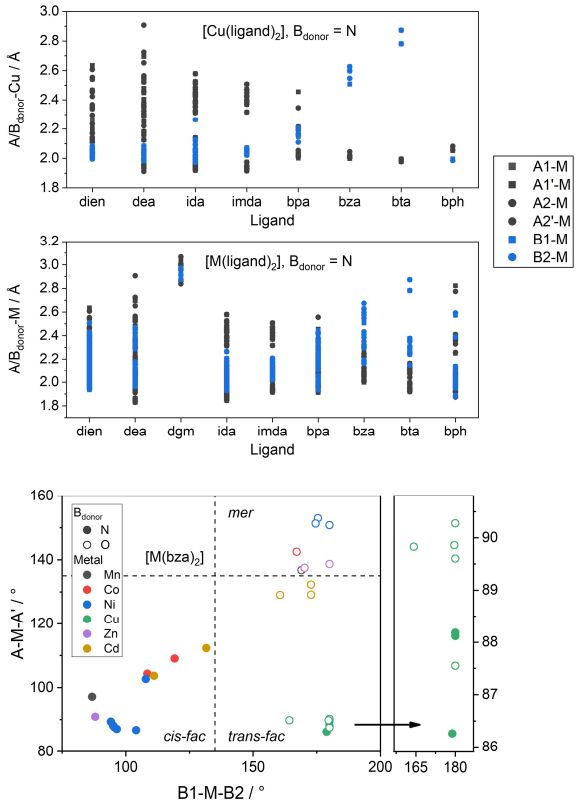

Figure 19. A/B_{donor}-M bond lengths for ligands with B_{donor} = N, for Cu(II) complexes (top) and all complexes (middle). Scatter plot of A-M-A' *vs.* B1-M-B2 angles for 16 **N-bza** and 15 **O-bza** ligands (bottom).

Although heterocyclic ligands **bpa** and **bza** showed a standard preference for *cis-fac* (for B_{donor} = N and R ≠ H), **bta** complexes are exclusively found as *trans-fac* isomers. Possibly the elongated B_{donor}-M bonds found in **bta** complexes support the *trans-fac* preference; however, the low diversity of reported **bta** complexes should be noted, as the relatively small number of **bta** ligands are mostly studied as part of the same series of compounds, adding to the similar isomer preferences.

5.2. Influence of the ligand

In the studies of Searle and Keene, mixtures of all three isomers were always found for **$[Co(dien)_2]^{3+}$** complexes.[6] On the other hand, Searle and Larsen[130] tried to determine the isomer ratios for **$[Co(S\text{-}dien)_2]^{3+}$** and found that if the central donor N atom was replaced by S, despite their

attempts to obtain *mer* and *trans-fac*, only the *cis-fac* isomer was obtained, indicating influence of the donor atom type on the isomeric preferences.[131]

Tridentate ligands corresponding to the general search are found with B_{donor} = N, P, O, S and Se atoms (Figure 20). If all the structures are analyzed according to the type of B_{donor} atom, for the most extensively used B_{donor} = N, all three isomers are equally represented. For the somewhat harder B_{donor} = O, *mer* and *trans-fac* isomers are found, while for the softer B_{donor} = S, *cis-* and *trans-fac* are found. For the even softer B_{donor} = P, only *cis-fac* is found, indicating that in general, ligands with hard B_{donor} atoms preferably form *mer*, while ligands with soft B_{donor} preferably form *cis-fac* isomers. Intermediate B_{donor} atoms adopt different configurations, with a prevalence of *trans-fac*. This is not surprising since combinations of soft acids and bases form covalent complexes that are more likely to have trigonal prismatic geometry, which is more convenient for *cis-fac* isomers. On the other hand, combinations of hard acids and bases form ionic complexes[122,132] that would ideally adopt octahedral geometry,[25] but in the case of *mer*, that is not possible due to the limited ligand bite. The *trans-fac* isomer is best suited for octahedral geometry.

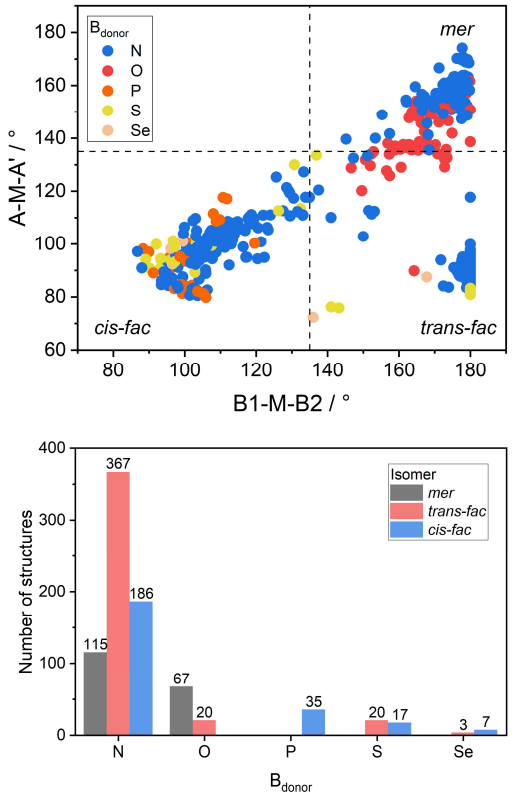

Figure 20. Scatter plot of A-M-A' *vs.* B1-M-B2 angles (top) and distribution of isomers (bottom) for all 844 **[M(ligand)$_2$]** complexes according to the type of B_{donor} atom. A few examples were found with B_{donor} atoms B (ROJMAH[133]), C (FUHBIV[134]), and Si (IRIFAS[135] and ESELEU[136]), but are not shown here due to the limited number of examples.

While N and O only act as σ-donors, P and S can also act as π-acceptors, further contributing to the covalent nature of the complex. Hoffman stated that octahedral geometry is often preferred due to ligand-ligand repulsions, while trigonal prismatic geometry is possibly stabilized by donation from the π-orbitals of the ligands, i.e., π-bonding has a significant role in the stabilization of trigonal prismatic geometry.[38,70,137]

Pandiyan and coworkers[138] studied the stereochemistry of **dien** and **bza** complexes by comparing B_{donor} = N and S, as well as amine compared to benzimidazole terminal donor groups. They observed that for cobalt complexes with **dien** ligands, the *mer* isomer is preferred, but with benzimidazole (**bza**) or pyridyl, generally *fac* isomers are preferred. This was consistent with the observation that *fac* isomers were preferred when terminal donors (arms) of the tridentate ligands were partially rigid and had reduced σ-donor and enhanced π-bonding ability. Another reason for *fac*

coordination was the soft central donor atom in the thioether. The thioether sulfur atom is both a weak σ-donor and a weak π-acceptor, while the amine nitrogen is a purely σ-donor atom. Kojima, Matsuda,[35] and Wolny[139] studied Ru(II) complexes of **bpa** ligands that formed *cis-fac* isomers. The authors stated that a possible cause of *cis-fac* coordination could be the *trans* effect of the σ-donating sp^3 nitrogen, which leads to coordination of the tertiary nitrogens *cis* to each other. The different electronic nature of the aliphatic and aromatic donor atoms is a possible cause of distortion from ideal octahedral geometry and could be one reason why heterocyclic ligands generally prefer *cis-fac* coordination.[31]

Galindo and coworkers[140] studied complexes of **ida** derivatives, oxydiacetate and thiodiacetate and their preferences for *mer* (planar) or *fac* (folded) coordination in cobalt complexes of ML stoichiometry. These preferences depend on the central B_{donor} atom, O or S, with both coordination modes achievable with oxydiacetate, while thiodiacetate gave exclusively the *fac* isomer. They analyzed several geometric parameters, stating that ligand folding (facial coordination) can be related to longer B_{donor}-M distances[39] and to the flexibility of the C-B_{donor}-C angle, where C is the carbon adjacent to the B_{donor} atom. These values are in turn dependent on parameters such as the hard/soft character, electronegativity and size of the B_{donor} atom, ionic radius, oxidation and spin state of the metal. Their analysis showed that building a model with reasonable bond distances and angles for a *mer* coordinated thiodiacetate was not possible.

Herein, a similar analysis on our dataset showed that C-B_{donor}-C angles for ligands with different B_{donor} atoms have the following mean values: C-N-C (114.0°), C-O-C (116.0°), C-P-C (105.1°), C-S-C (104.0°), and C-Se-C (102.3°). The differences between C-B_{donor}-C angles of the three isomers are not large; however, the values for *mer* (115.9°) are larger than for *trans*- (113.0°) and *cis-fac* (111.69°). Considering these values, it is expected that the *mer* isomer would be highly strained for ligands with B_{donor} = S, P, or Se.[141]

Increasing the B_{donor} atomic size leads to longer B_{donor}-M distances. Considering the ligand bite angles, long B_{donor}-M distances in a *mer* isomer would lead to a severely distorted coordination geometry. Such irregular geometries were observed in K^+ complexes, where all coordination bonds are elongated compared to other analyzed complexes due to the large size of K^+. Therefore, it would be expected that for larger B_{donor} atoms, it is difficult to achieve planar (*mer*) coordination of the ligand. Indeed, no *mer* ML_2 complexes are reported for ligands with B_{donor} = P, S, or Se.

In addition, we analyzed the *mer*/*fac* coordination mode of tridentate ligands shown in Figure 1 in complexes of ML stoichiometry (

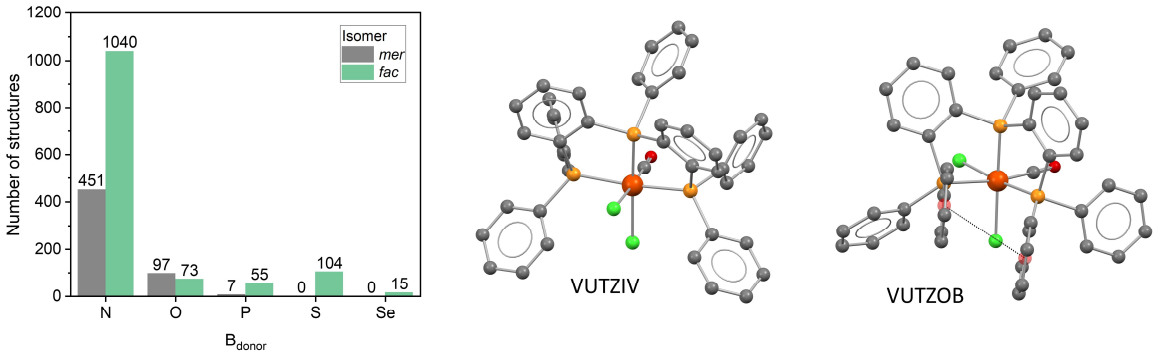

Figure 21). In 1928 analyzed ML complexes of tridentate ligands, similar as in ML_2 complexes, meridional coordination was not observed for B_{donor} = S or Se. However, unlike in ML_2 complexes, the *mer* isomer was observed for a small number of ligands with B_{donor} = P. The seven *mer* complexes with B_{donor} = P are **bph** ligands with sterically demanding substituents on the A_{donor} atoms. The steric requirements of those substituents, such as two phenyl rings or isopropyl, possibly render the *fac* configuration less stable. ML complexes *mer*-**[Fe(bph)(CO)(Cl)$_2$]** (VUTZIV) and *fac*-**[Fe(bph)(CO)(Cl)$_2$]** (VUTZOB) described by Dzik et.al.[142] are examples of a *mer-fac* switch that can

be controlled by photo- and thermal stimuli (

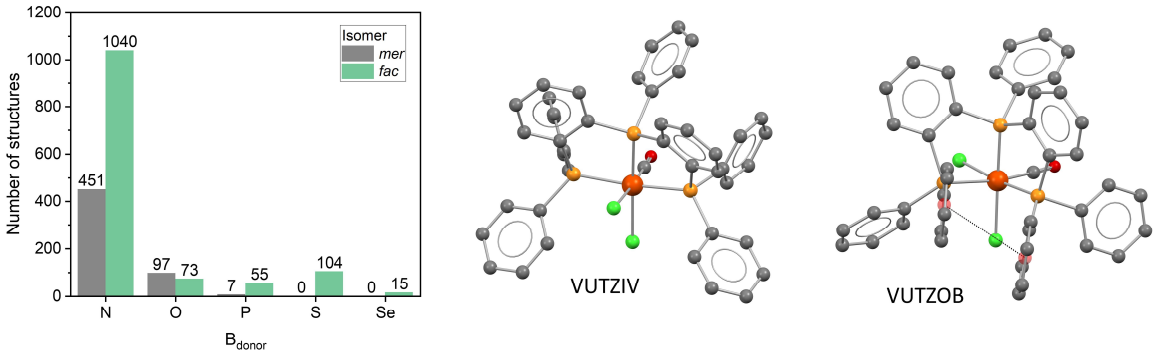

Figure 21).

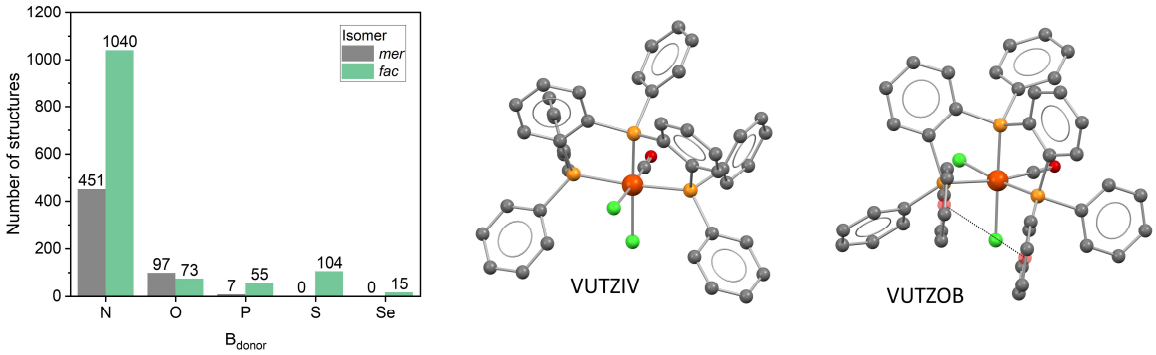

Figure 21. Distribution of *mer* and *fac* isomers for 1928 ML complexes of tridentate ligands with different B_{donor} atoms. Several structures are reported with B_{donor} = C, B, Si, As, and Te, but they are not shown here due to the limited number of examples. Structures *mer*-VUTZIV and *fac*-VUTZOB.

The A/B_{donor}-M bond lengths depend on the size of the metal cation and donor atoms. Figure 22 shows dependence of the A1-B1-B2-A1' dihedral angle on the average value of the six A/B_{donor}-M bond lengths for the 844 **[M(ligand)$_2$]** complexes. The A1-B1-B2-A1' dihedral angle can be used to distinguish the three isomers, and the average values of the bond lengths contain contributions of the metal ion size and sizes of all the donor atoms in the form of their interatomic distances. As the bond lengths increase, the dihedral angles deviate from the ideal values for the three isomers (Figure 22). The distortion parameter Σ shows that these increased values also lead to distortion from octahedral geometry.

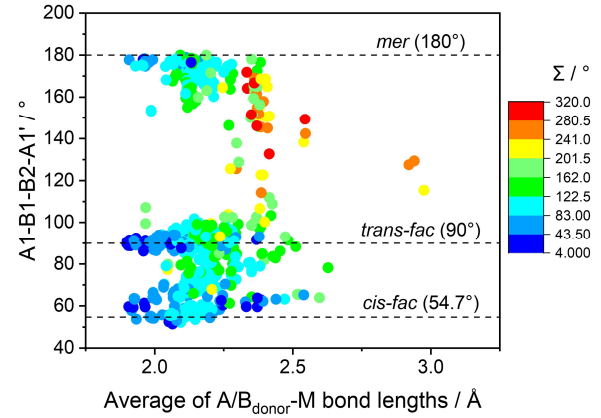

Figure 22. Dependence of the A1-B1-B2-A1' dihedral angle on the A/B_{donor}-M bond lengths for 844 **[M(ligand)$_2$]** complexes. Each complex has two dihedral angle values (A1-B1-B2-A1' and A2-B2-B1-A2') so their average value was used in the analysis.

The substituent R (tail) on the central B_{donor} = N or P atoms allows further modifications of the system, such as introducing additional donor atoms or chiral elements. Here we focused mainly on this influence for B_{donor} = N ligands, as for B_{donor} = P, the options found in the literature are somewhat limited to R = phenyl or a third equivalent terminal donor group (arm). For B_{donor} = N, a large dataset is available for various R groups. For R = H, there is also the possibility of deprotonation, as was observed for some **bpa** and **bph** complexes. In this case, the central N atom has an additional lone pair and can be compared to B_{donor} = O, with a preference for meridional coordination. In some of the deprotonated ligands, delocalization of the bonds next to the central N atom occurred, further contributing to the planar conformation of the ligand. For R ≠ H, R can be a simple alkyl or aryl group, or a group containing an additional donor atom; often a third equivalent donor group as in tripodal ligands. N-methylation of the B_{donor} nitrogen favors trigonal coordination of the tertiary nitrogen due to the increased bond angle strain compared to the H-ligand, favoring facial coordination for N-methylated ligands.[143]

For all ligands, a trend was observed that complexes with R-ligands have a distinct preference for a certain isomer, while H-ligands were stereochemically more diverse and usually had no apparent preference (Figure 23). There could be several reasons for this; the smaller size and different electronic properties of H compared to R groups, the possibility of hydrogen bonding, easier isomerization, and influence of pH. Considering the specific properties of R = H, it is not surprising that the H-ligands show such stereochemical diversity compared to R-ligands. Therefore, the preference observed for the R-ligands can be considered the standard preference for a particular type of ligand with B_{donor} = N. If only R-ligands are considered, it appears that ligands with functional groups as terminal donor sites (**dien**, **dea**, **ida**, **imda**) give *trans-fac*, while heterocyclic ligands (**bpa**, **bza**) give *cis-fac*, with the exception of **bta** ligands. A possible reason for these preferences is that in general, complexes of transition metals and functional group donor atoms are harder, forming more ionic complexes, while heterocyclic donors are softer bases and form more covalent complexes.

If the larger dipole moment of *cis-fac* compared to the centrosymmetric *trans-fac* isomer is considered, *trans-fac* complexes are expected to be less soluble in water and therefore more readily isolated from an aqueous environment.[79] Furthermore, complexes of functional group ligands are often studied in aqueous environments, while complexes of heterocyclic ligands are studied in organic solvents, indicating that the type of solvent used could support the more frequent isolation of *trans-fac* isomers for functional group and *cis-fac* isomers for heterocyclic ligands. We attempted to study this influence for labile Co(II) and Ni(II) complexes of H-dien ligands that have a significant number of all three isomers reported. However, many of these complexes were prepared by the solvothermal method as a part of larger inorganic structures and when these structures were disregarded, the remaining dataset was not sufficient for observing a trend in the solvent influence.

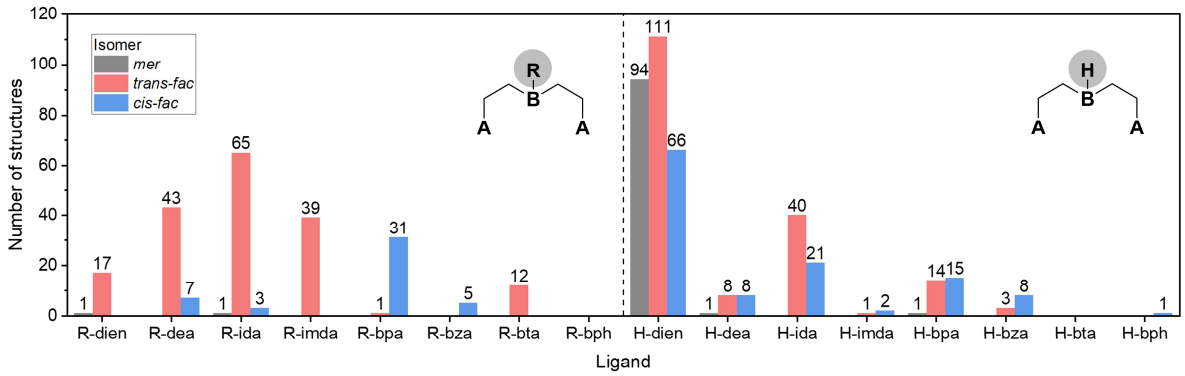

Figure 23. Distribution of isomers showing the uniform isomer preferences of R-ligands and non-uniform preferences of H-ligands for ligands with B_{donor} = N.

A small number of **[M(R-ligand)$_2$]** complexes differ from the observed R-ligand preferences (

Table 2). The trigonal prismatic geometry of Ti(IV) complexes DEJXIA and XEXKUG and Hg(II) complex BELNOX makes their isomer classification somewhat ambiguous. In **R-ida** complexes CEDGEX, JUKNUY, and LETXIS, interactions of the carbonyl group with metal cations could influence the isomer preferences. A common motif here is the small R = methyl group that possibly leads to a smaller energy difference between isomers.

Table 2. **[M(R-ligand)$_2$]** complexes that differ from the observed R-ligand preference for a particular ligand.

Refcode	Metal ion	Ligand	R	Isomer	Reference
UFEQOL	Co(III)	**R-dien**	CH_3	*mer*	[55]
DEJXIA[a]	Ti(IV)	**R-dea**[c]	CH_2-Ph	*cis-fac*	[144]
ETAMSN[b]	Sn(IV)	**R-dea**[c]	$(CH_2)_2$-OH	*cis-fac*	[145]
ONENAX[a]	Sn(IV)	**R-dea**[c]	CH_3	*cis-fac*	[146]
XEXKUG	Ti(IV)	**R-dea**[c]	CH_3	*cis-fac*	[147]
CEDGEX	Co(III)	**R-ida**	CH_3	*cis-fac*	[148]
JUKNUY	Co(III)	**R-ida**	CH_3	*cis-fac*	[149]
LETXIS	Fe(III)	**R-ida**	CH_3	*mer*	[29]
DUJJOK	Cu(II)	**R-ida**	3,5-dicarboxyphenyl	*cis-fac*	[150]
BELNOX	Hg(II)	**R-bpa**	CH_3	*trans-fac*	[84]

[a]Two complex cations in the crystal structure, [b]both structures ETAMSN and ETAMSN01 are considered in Figure 23, [c]deprotonated

In our recent studies of **[M(imda)$_2$]** complexes, variable temperature NMR studies and DFT calculations showed that the electron-donating ability of R on B_{donor} influenced the B_{donor}-M bond strength and the isomer preference. The strength of the B_{donor}-Zn bond decreased for substituents R in the order *i*Pr > Bn > Me ≈ H. Substitution with the smallest R = H gave the narrowest range of differences in energy between the three isomers.[34]

Keene and Searle[151] described possible isomerization mechanisms of **[Co(dien)$_2$]$^{3+}$**; by intramolecular twists or bond ruptures, and they compared isomerization reactions of **[Co(H-dien)$_2$]$^{3+}$** and mixed **[Co(H-dien)(R-dien)]$^{3+}$** complexes. They proposed that the isomerization reactions are base-catalyzed and probably involve conjugate-base intermediates, deprotonated at the secondary amine nitrogen atoms (B_{donor}) of coordinated **dien** ligands. Kawaguchi[152] studied the isomerization mechanisms of **[Co(ida)$_2$]$^-$** complexes, showing that the base-catalyzed mechanism is best explained by a transient five coordinated conjugate base intermediate formed by bond rupture. However, the possibility of the twist mechanism should also be considered.

Ligands that have an additional donor atom in the side chain R, such as tripodal ligands with three identical donor groups, can act as tetradentate ligands. Tetradentate coordination in ML complexes during synthesis could influence the reaction mechanism of formation of ML_2 complexes, as observed by Zhu et.al.[10], where they compared two **bpa** ligands with different coordination possibilities of the chain R; the 1,5-substituted triazole as a passive linker and the 1,4-substituted triazole as a chelatable group (Figure 24). The *cis-fac*-**[M(R-bpa)$_2$]** complex (LIHYAE) of the 1,5-substituted ligand was isolated in the solid-state and was also observed in acetonitrile-d_3 solution by ^{1}H NMR spectroscopy. For the 1,4-substituted ligand, ^{1}H NMR showed that the chelatable 1,2,3-triazolyl group may aid the ligand exchange and accelerate the equilibrium between the ML_2 and ML complexes. Isothermal titration calorimetry (ICT) further supported these results, showing the equilibrium constant from the ML to ML_2 complex was over an order of magnitude larger for the 1,5-substituted ligand without the possibility of coordination of chain R.

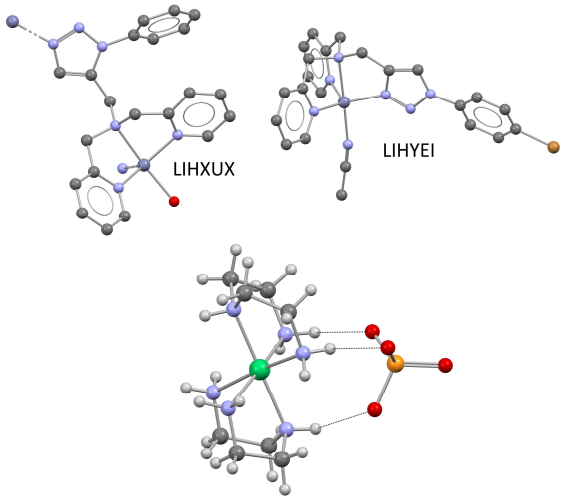

Figure 24. Structure LIHXUX with a 1,5-substituted triazole group and LIHYEI with a 1,4-substituted triazole group.[10] Proposed non-covalent interactions of a *trans-fac* isomer with a PO_4^{3-} anion, modified from [5] using crystallographic data from XENDAV.[50]

Although there is an apparent influence of the R group with a donor atom on the kinetics of the reaction observed in solution, in the analysis of crystal structures, the isomer preferences of R-ligands appear to be consistent for all R (R≠H) groups, regardless of the presence of an additional donor atom. Alongside the electronic properties, the steric properties of the R group can also be important. It would be expected that ligands with bulky R groups prefer *trans-fac* or *mer* to avoid steric repulsions in the *cis-fac* complex. Although this influence cannot be ignored, there are many examples where *cis-fac* was obtained despite the steric bulkiness of the R group.[35,153]

Interestingly, for **H-dien** and **H-bpa** ligands, complexes were found that contain two or even all three isomers in the same crystal structure, for example, KUTNES[154] and WOZLIG[155]. Twenty-five such structures were found for **H-dien** and three for **H-bpa** complexes. Such structures were not found for any of the other analyzed ligands. This observation could be correlated to the similarity of the terminal donor atoms and the central donor atom in **dien**, leading to a small energy difference between the three isomers for these ligands. Generally, larger differences in the electronic properties of the A_{donor} and B_{donor} atoms lead to more pronounced isomer preferences.[156] Earlier studies showed that the energy differences between the three isomers of **dien** complexes are only a few kJ mol^{-1} and that thermally induced isomerization would be possible. Chaudhuri and coworkers[157] showed that a **$[Ni(dien)_2](SCN)_2$** complex undergoes a phase transition involving a low-temperature ordered system (*trans-fac*-HENNET) and a high-temperature disordered system (*mer*-HENNIX). The metastable *mer* isomer was also isolated from the solution and would isomerize into the *trans-fac* isomer in a humid atmosphere.

5.3. Influence of ion association

The influence of various factors such as ion association, solvation, temperature, and non-covalent interactions on the isomer distribution was studied by Keene and Searle for the complex system **$[Co(dien)_2]^{3+}$**.[5] The changes of various factors led to changes in the geometric isomer distributions, measured by chromatographic separations of the isomers. Under the usual preparative conditions, in aqueous solutions and with strongly coordinating anions (Cl^-, Br^-), at 18°C, they obtained **$[Co(dien)_2]^{3+}$** isomers in ratios *trans-fac* : *cis-fac* : *mer* = 7 : 28 : 65. The larger preference for *cis-fac* compared to *trans-fac* was due to statistical reasons; two possible ways of coordination of the second ligand in *cis-fac*, compared to only one possible way in *trans-fac*. Compared to anions with a single negative charge, larger association effects are expected for highly charged oxyanions. Addition of oxyanions SO_4^{2-}, SeO_3^{2-}, PO_4^{3-}, and HPO_4^{2-} had a significant influence on the isomer distribution, making *trans-fac* more stable at the expense of *mer*, while the proportion of *cis-fac* remained nearly

constant. This suggested specific interactions between the anion (Figure 24), namely PO_4^{3-} and the three isomers, in the order *trans-fac* > *cis-fac* > *mer*. The NH groups of the *cis-fac* and *mer* isomer are in a less favorable position for such hydrogen bonds.

Yoshikawa and coworkers described the chromatographic separation of the three isomers of **$[Co(dien)_2]^{3+}$**.[158] Interactions of the complex cation with the eluent anion had a significant influence on the separation of isomers. This was correlated with the number and kind of octahedral faces of the **$[Co(dien)_2]^{3+}$** cation available for ion association with oxo anions such as phosphate. The described tendency for ion-pair formation was: *trans-fac* > *cis-fac* > *mer*, which was in agreement with the experimentally observed elution order and the ion-association preferences described by Keene and Searle.[5]

6. Conclusions

In this review, we analyzed the stereochemistry of 844 bis-tridentate ligand complexes found in the CSD database. In the analysis of *mer*, *trans-fac*, and *cis-fac* isomer preferences, several trends were observed regarding the type of metal cation, choice of donor atoms in the ligand, the possibility of non-covalent interactions, etc. These trends are only qualitative, however, simplified guidelines can be provided, as shown in Table 3.

Table 3. A simplified representation of influences on the stereochemistry of **$[M(A\text{-}B\text{-}A)_2]$** complexes.

Isomer	Metal ion	B_{donor}	Bond character	Arm (A_{donor} group)	Tail (R)	Geometry
mer	hard	hard	ionic	-	deprotonated R = H	distortion of the A-M-A' angle
trans-fac	intermediate	intermediate	intermediate	functional group (hard)	uniform preference for R ≠ H; variable preference for R = H	octahedral
cis-fac	soft	soft	covalent	heterocyclic (soft)	uniform preference for R ≠ H; variable preference for R = H	distortion of the B1-M-B2 angle

The *mer* isomer is most readily obtained with combinations of hard B_{donor} atoms, such as O, and hard metal cations, such as s-block metals. The formation of octahedral geometry expected for ionic complexes is distorted by the ligand bite angle in the *mer* isomer. The *cis-fac* configuration, often with a distorted B1-M-B2 angle, is best suited for trigonal prismatic geometry, which is most readily obtained for covalent complexes, for example, combinations of soft B_{donor} atoms, such as P, S, and Se, and soft 4d and 5d metals. The *trans-fac* isomer enables nearly ideal octahedral geometric parameters and is generally found for intermediate-intermediate combinations of ligands and metals.

Considering the type of ligand, for the most common case of B_{donor} = N, functional group ligands (**dien**, **dea**, **ida**, **imda**), with hard A_{donor} groups (arms) generally prefer *trans-fac* coordination. On the other hand, ligands with A_{donor} atoms as part of a heterocyclic ring (**bpa**, **bza**) are mostly found as *cis-fac* isomers. The third substituent on the central N atom, R (tail), has a significant influence on the energy difference between the three isomers. Ligands with R = alkyl or aryl have more predictable stereochemical preferences, while ligands with R = H often lead to small energy differences between isomers and are more dependant on external conditions such as pH, π-π interactions in ligands with aromatic rings, or non-covalent interactions with the counterion. Deprotonation of the central B_{donor} = N atom often leads to the formation of a conjugated system imposing planarity of the ligand and formation of *mer* isomers.

Understanding the stereochemistry of coordination compounds is essential when designing complexes for various applications. The many factors described herein are often mutually dependent,

and quantitative evaluation of a specific influence is often not possible. However, we believe that the overview of factors provided here can serve as a starting point in the rational design of a **[M(A-B-A)$_2$]** system suitable for a specific use. We hope this review will instigate further experimental and theoretical studies of tridentate ligand systems, to broaden the crystal structure dataset with information about the complexes in solution. Current studies of these systems, with applications as structure directing cations, models for bioinorganic systems etc., would definitely benefit from such findings.

Acknowledgment

This work was partially supported by CAT Pharma (KK.01.1.1.04.0013), a project co-financed by the Croatian Government and the European Union through the European Regional Development Fund - the Competitiveness and Cohesion Operational Programme, and Minimal Artificial Enzymes (IP-2014-09-1461), a project financed by the Croatian Science Foundation.

Supplementary material

A supplementary file containing geometrical parameters used in the analyses can be found at doi:

7. References

[1] E.L. Eliel, S.H. Wilen, Stereochemistry of Organic Compounds, Wiley India Pvt. Limited, 2008.
[2] A. von Zelewsky, Stereochemistry of Coordination Compounds, John Wiley & Sons, Ltd, 1996.
[3] H. Amouri, M. Gruselle, Chirality in Transition Metal Chemistry, John Wiley & Sons, Ltd, 2008.
[4] F.G. Mann, 108. The constitution of complex metallic salts. Part II. The platinum derivatives of ββ′-diaminodiethylamine, J. Chem. Soc. (1934) 466–474. https://doi.org/10.1039/JR9340000466.
[5] F.R. Keene, G.H. Searle, Isomers of the bis(diethylenetriamine)cobalt(III) cation. Dependence of equilibrium isomer proportions on environmental parameters, Inorg. Chem. 13 (1974) 2173–2180. https://doi.org/10.1021/ic50139a023.
[6] F.R. Keene, G.H. Searle, Y. Yoshikawa, A. Imai, K. Yamasaki, Geometric and optical isomers of the bis(diethylenetriamine)cobalt(III) ion, J. Chem. Soc. D Chem. Commun. (1970) 784–786. https://doi.org/10.1039/C29700000784.
[7] Y. Yoshikawa, K. Yamasaki, Isomerism of the Metal Complexes containing Multidentate Ligands. I. Geometric and Optical Isomers of the Bis(diethylenetriamine)-cobalt(III) Ion, Bull. Chem. Soc. Jpn. 45 (1972) 179–184. https://doi.org/10.1246/bcsj.45.179.
[8] A. Ehnbom, S.K. Ghosh, K.G. Lewis, J.A. Gladysz, Octahedral Werner complexes with substituted ethylenediamine ligands: a stereochemical primer for a historic series of compounds now emerging as a modern family of catalysts, Chem. Soc. Rev. 45 (2016) 6799–6811. https://doi.org/10.1039/C6CS00604C.
[9] S.L. Dabb, N.C. Fletcher, mer and fac isomerism in tris chelate diimine metal complexes, Dalton Trans. 44 (2015) 4406–4422. https://doi.org/10.1039/C4DT03535F.
[10] J.T. Simmons, J.R. Allen, D.R. Morris, R.J. Clark, C.W. Levenson, M.W. Davidson, L. Zhu, Integrated and passive 1,2,3-triazolyl groups in fluorescent indicators for zinc(II) ions: thermodynamic and kinetic evaluations, Inorg. Chem. 52 (2013) 5838–5850. https://doi.org/10.1021/ic302798u.
[11] S. Anjana, S. Donring, P. Sanjib, B. Varghese, N.N. Murthy, Controlling the oxidation of bis-tridentate cobalt(II) complexes having bis(2-pyridylalkyl)amines: ligand vs. metal oxidation, Dalton Trans. 46 (2017) 10830–10836. https://doi.org/10.1039/C7DT01792H.
[12] W. Liu, D. Zhong, C.-L. Yu, Y. Zhang, D. Wu, Y.-L. Feng, H. Cong, X. Lu, W.-B. Liu, Iron-Catalyzed

Intramolecular Amination of Aliphatic C–H Bonds of Sulfamate Esters with High Reactivity and Chemoselectivity, Org. Lett. 21 (2019) 2673–2678. https://doi.org/10.1021/acs.orglett.9b00660.
[13] D. Schweinfurth, S. Demeshko, S. Hohloch, M. Steinmetz, J.G. Brandenburg, S. Dechert, F. Meyer, S. Grimme, B. Sarkar, Spin Crossover in Fe(II) and Co(II) Complexes with the Same Click-Derived Tripodal Ligand, Inorg. Chem. 53 (2014) 8203–8212. https://doi.org/10.1021/ic500264k.
[14] C. Tang, F. Wang, W. Jiang, Y. Zhang, D. Jia, Clusters [Co(As3S3)2]2–, [Ni(As3S3)2]2–, and [{Co(en)}6(μ3-S)4(AsS3)4]2– with Co–As or Ni–As Bonds: Solvothermal Syntheses and Characterizations of Thioarsenates Containing Transition-Metal Complexes, Inorg. Chem. 52 (2013) 10860–10868. https://doi.org/10.1021/ic4007982.
[15] D.Y. Shopov, B. Rudshteyn, J. Campos, V.S. Batista, R.H. Crabtree, G.W. Brudvig, Stable Iridium(IV) Complexes of an Oxidation-Resistant Pyridine-Alkoxide Ligand: Highly Divergent Redox Properties Depending on the Isomeric Form Adopted, J. Am. Chem. Soc. 137 (2015) 7243–7250. https://doi.org/10.1021/jacs.5b04185.
[16] J. Mola, M. Rodríguez, I. Romero, A. Llobet, T. Parella, A. Poater, M. Duran, M. Solà, J. Benet-Buchholz, New Ru Complexes Containing the N-Tridentate bpea and Phosphine Ligands: Consequences of Meridional vs Facial Geometry, Inorg. Chem. 45 (2006) 10520–10529. https://doi.org/10.1021/ic061126l.
[17] M.C. Favas, D.L. Kepert, Stereochemistry of six-co-ordinate bis(tridentate ligand)metal complexes, J. Chem. Soc. Dalton Trans. (1978) 793–797. https://doi.org/10.1039/DT9780000793.
[18] D.L. Kepert, Inorganic Stereochemistry, Springer-Verlag Berlin Heidelberg New York, 1982. https://doi.org/10.1007/978-3-642-68046-5.
[19] C.R. Groom, I.J. Bruno, M.P. Lightfoot, S.C. Ward, The Cambridge Structural Database, Acta Cryst. 72 (2016) 171–179. https://doi.org/10.1107/S2052520616003954.
[20] E. Peris, R.H. Crabtree, Key factors in pincer ligand design, Chem. Soc. Rev. 47 (2018) 1959–1968. https://doi.org/10.1039/C7CS00693D.
[21] A.G. Orpen, Structural systematics in molecular inorganic chemistry, Chem. Soc. Rev. 22 (1993) 191–197. https://doi.org/10.1039/CS9932200191.
[22] G.H. Searle, D.A. House, The Isomers of the Bis(Diethylenetriamine)Chromium(III) and Bis[Di(3-Aminopropyl)Amine]Chromium(III) Cations, [Cr(Dien)2]3+ and [Cr(Dpt)2]3+: Preparation and Characterization, Aust. J. Chem. 40 (1987) 361–374. https://doi.org/10.1071/CH9870361.
[23] G.L. Miessler, P.J. Fischer, D.A. Tarr, Inorganic Chemistry, Pearson Education, 2013.
[24] V. Rodríguez, J.M. Gutiérrez-Zorrilla, P. Vitoria, A. Luque, P. Román, M. Martínez-Ripoll, Synthesis, vibrational study, crystal structure and density functional calculations of [Ni(dien)2]2+ complexes. Configurational and conformational study of [M(dien)2]n+ complexes, Inorg. Chim. Acta. 290 (1999) 57–63. https://doi.org/10.1016/S0020-1693(99)00115-2.
[25] E. Cremades, J. Echeverría, S. Alvarez, The Trigonal Prism in Coordination Chemistry, Chem. Eur. J. 16 (2010) 10380–10396. https://doi.org/10.1002/chem.200903032.
[26] J. Cipressi, S.N. Brown, Octahedral to trigonal prismatic distortion driven by subjacent orbital π antibonding interactions and modulated by ligand redox noninnocence, Chem. Commun. 50 (2014) 7956–7959. https://doi.org/10.1039/C4CC03404J.
[27] C. Andreini, G. Cavallaro, S. Lorenzini, FindGeo: a tool for determining metal coordination geometry, Bioinformatics. 28 (2012) 1658–1660. https://doi.org/10.1093/bioinformatics/bts246.
[28] F.R. Keene, G.H. Searle, Isomers of the bis(diethylenetriamine)cobalt(III) ion and a new source of optical activity, Inorg. Chem. 11 (1972) 148–156. https://doi.org/10.1021/ic50107a033.
[29] R. Meier, M. Molinier, C. Anson, A.K. Powell, B. Kallies, R. van Eldik, Structure of sodium

bis(N-methyl-iminodiacetato)iron(III): trans-meridional N-coordination in the solid state and in solution, Dalton Trans. (2006) 5506–5514. https://doi.org/10.1039/B605056E.
[30] K. Harada, The Synthesis and X-Ray Crystal Structures of Bis(diethylenetriamine)rhodium(III), Bis(diethylenetriamine)iridium(III), and Bis[bis(3-aminopropyl)amine]rhodium(III) Complexes, Bull. Chem. Soc. Jpn. 66 (1993) 2889–2899. https://doi.org/10.1246/bcsj.66.2889.
[31] I. Romero, M. Rodríguez, A. Llobet, M.-N. Collomb-Dunand-Sauthier, A. Deronzier, T. Parella, H. Stoeckli-Evans, Synthesis, structure and redox properties of a new ruthenium(II) complex containing the flexible tridentate ligand N,N-bis(2-pyridylmethyl)ethylamine, cis-fac-Ru(bpea)22+, and its homologue attached covalently to a polypyrrole film , J. Chem. Soc. Dalton Trans. (2000) 1689–1694. https://doi.org/10.1039/A909511J.
[32] G.H. Searle, S.F. Lincoln, F.R. Keene, S.G. Teague, D.G. Rowe, Bis(tridentate)cobalt(III) complexes with diethylenetriamine and 4-Methyldiethylenetriamine [2,2'-Methyliminodi(ethylamine)]: Assignment of geometric configurations by 1H and 13C N.M.R. spectroscopy, Aust. J. Chem. 30 (1977) 1221. https://doi.org/10.1071/ch9771221.
[33] K.A. Jensen, Tentative proposals for nomenclature of absolute configurations concerned with six-coordinated complexes based on the octahedron, Inorg. Chem. 9 (1970) 1–5. https://doi.org/10.1021/ic50083a001.
[34] N. Pantalon Juraj, G. Miletić, B. Perić, Z. Popović, N. Smrečki, R. Vianello, S.I. Kirin, Stereochemistry of Hexacoordinated Zn(II), Cu(II), Ni(II) and Co(II) Complexes with Iminodiacetamide Ligands, Inorg. Chem. 58 (2019) 16445–16457. https://doi.org/10.1021/acs.inorgchem.9b02200.
[35] T. Kojima, Y. Matsuda, Chiral induction upon coordination to form an enantiomeric bis-chelate ruthenium(II)–tris(3-methyl-2-pyridylmethyl)amine complex, J. Chem. Soc. Dalton Trans. (2001) 958–960. https://doi.org/10.1039/B100095K.
[36] M. Lenze, E.T. Martin, N.P. Rath, E.B. Bauer, Iron(II) α-Aminopyridine Complexes and Their Catalytic Activity in Oxidation Reactions: A Comparative Study of Activity and Ligand Decomposition, Chempluschem. 78 (2013) 101–116. https://doi.org/10.1002/cplu.201200244.
[37] P. Osvath, A. Oliver, A.G. Lappin, Stereosopecificity in [Co(sep)][Co(edta)]Cl2·2H2O, Chemistry. 3 (2021) 228–237. https://doi.org/10.3390/chemistry3010017.
[38] A.A. Diamantis, M. Manikas, M.A. Salam, M.R. Snow, E.R.T. Tiekink, The Relationship Between Octahedral and Trigonal-Prismatic Coordination in Bis Tridentate Complexes of Ti^{IV} and V^{IV}, Aust. J. Chem. 41 (1988) 453–468. https://doi.org/10.1071/CH9880453.
[39] D. del Río, A. Galindo, R. Vicente, C. Mealli, A. Ienco, D. Masi, Synthesis, molecular structure and properties of oxo-vanadium(IV) complexes containing the oxydiacetate ligand, Dalton Trans. (2003) 1813–1820. https://doi.org/10.1039/B300914A.
[40] E. Bouwman, B. Douziech, L. Gutierrez-Soto, M. Beretta, W.L. Driessen, J. Reedijk, G. Mendoza-Díaz, Co(II), Ni(II), and Zn(II) compounds of the new tridentate ligand N,N-bis(2-ethyl-5-methyl-imidazol-4-ylmethyl)aminopropane (biap). X-ray structures of biap·H2O, [Co(biap)(NCS)(OAc)], [Ni(biap)(NCS)(OAc)], [Ni(biap)(NCS)2(MeCN)](MeCN), and [Ni(biap)2](BF4, Inorg. Chim. Acta. 304 (2000) 250–259. https://doi.org/10.1016/S0020-1693(00)00097-9.
[41] J. Septavaux, C. Tosi, P. Jame, C. Nervi, R. Gobetto, J. Leclaire, Simultaneous CO2 capture and metal purification from waste streams using triple-level dynamic combinatorial chemistry, Nat. Chem. 12 (2020) 202–212. https://doi.org/10.1038/s41557-019-0388-5.
[42] P.C. Junk, J.W. Steed, A structural study of late transition metal diethylenetriamine complexes, Inorg. Chim. Acta. 360 (2007) 1661–1668. https://doi.org/10.1016/j.ica.2006.09.001.
[43] C. Heering, B. Francis, B. Nateghi, G. Makhloufi, S. Lüdeke, C. Janiak, Syntheses, structures and properties of group 12 element (Zn, Cd, Hg) coordination polymers with a mixed-functional phosphonate-biphenyl-carboxylate linker, CrystEngComm. 18 (2016) 5209–5223.

https://doi.org/10.1039/C6CE00587J.
[44] S. Banerjee, A. Ghosh, B. Wu, P.-G. Lassahn, C. Janiak, Polymethylene spacer regulated structural divergence in cadmium complexes: Unusual trigonal prismatic and severely distorted octahedral coordination, Polyhedron. 24 (2005) 593–599. https://doi.org/10.1016/j.poly.2005.01.005.
[45] M.A. Halcrow, Structure:function relationships in molecular spin-crossover complexes, Chem. Soc. Rev. 40 (2011) 4119–4142. https://doi.org/10.1039/C1CS15046D.
[46] P. Guionneau, M. Marchivie, G. Bravic, J.-F. Létard, D. Chasseau, Structural Aspects of Spin Crossover. Example of the [FeIILn(NCS)2] Complexes BT - Spin Crossover in Transition Metal Compounds II, in: P. Gütlich, H.A. Goodwin (Eds.), Springer Berlin Heidelberg, 2004: pp. 97–128. https://doi.org/10.1007/b95414.
[47] K. Robinson, G. V Gibbs, P.H. Ribbe, Quadratic Elongation: A Quantitative Measure of Distortion in Coordination Polyhedra, Science (80-.). 172 (1971) 567–570. https://doi.org/10.1126/science.172.3983.567.
[48] D. Cortecchia, S. Neutzner, A.R. Srimath Kandada, E. Mosconi, D. Meggiolaro, F. De Angelis, C. Soci, A. Petrozza, Broadband Emission in Two-Dimensional Hybrid Perovskites: The Role of Structural Deformation, J. Am. Chem. Soc. 139 (2017) 39–42. https://doi.org/10.1021/jacs.6b10390.
[49] C.-Y. Yue, X.-W. Lei, L.-J. Feng, C. Wang, Y.-P. Gong, X.-Y. Liu, [Mn2Ga4Sn4S20]8− T3 supertetrahedral nanocluster directed by a series of transition metal complexes, Dalton Trans. 44 (2015) 2416–2424. https://doi.org/10.1039/C4DT02864C.
[50] Y. Xu, D.-R. Zhu, Z.-J. Guo, Y.-J. Shi, K.-L. Zhang, X.-Z. You, Cation-induced assembly of the first mixed molybdenum–vanadium hexadecametal host shell cluster anions, J. Chem. Soc. Dalton Trans. (2001) 772–773. https://doi.org/10.1039/B010227J.
[51] D. Sun, D.-F. Wang, F.-J. Liu, H.-J. Hao, N. Zhang, R.-B. Huang, L.-S. Zheng, Design and synthesis of 3d–4d heterometallic coordination complexes based on a nonanuclear silver(I) metallatecton, CrystEngComm. 13 (2011) 2833–2836. https://doi.org/10.1039/C1CE05023K.
[52] Y. Wang, J. Yu, M. Guo, R. Xu, [{Zn2(HPO4)4}{Co(dien)2}]·H3O: A Zinc Phosphate with Multidirectional Intersecting Helical Channels, Angew. Chem. Int. Ed. 42 (2003) 4089–4092. https://doi.org/10.1002/anie.200351643.
[53] R. Stähler, C. Näther, W. Bensch, Solvothermal syntheses, crystal structures, and thermal stability of two new thioantimonates(III) using complex transition metal cations as structure directing agents: the layered compound [Ni(dien)2]Sb4S7·H2O and the three-dimensional compound [Ni(dien)2, J. Solid State Chem. 174 (2003) 264–275. https://doi.org/10.1016/S0022-4596(03)00216-0.
[54] H.-X. Zhang, J. Zhang, S.-T. Zheng, G.-Y. Yang, [Ge(7)O(13)(OH)(2)F(3)](3)(-).Cl(-).2[Ni(dien)(2)](2+): the first chainlike germanate templated by a transition metal complex, Inorg. Chem. 42 (2003) 6595–6597. https://doi.org/10.1021/ic034645m.
[55] T. Yasui, Y. Nishimoto, T. Yonemura, T. Ama, H. Kawaguchi, K. Okamoto, Preparation and Characterization of the Optically Active u-fac and mer Isomers of Bis(3-methyl-3-azapentane-1,5-diamine)cobalt(III) Ion, [Co(mdien)2]3+, and Crystal Structures of (-)CD536-mer and s-fac Isomers, Mem. Fac. Sci. Kochi Univ. Ser. C. Chem. 20 (1999) 1–15.
[56] A.M. Bond, F.R. Keene, N.W. Rumble, G.H. Searle, M.R. Snow, Polarographic studies of the geometric isomers of the bis(diethylenetriamine)cobalt(III) and -cobalt(II) cations in acetone, Inorg. Chem. 17 (1978) 2847–2853. https://doi.org/10.1021/ic50188a033.
[57] R. Yamaguchi, H. Sakiyama, Formation and decomposition of Nickel(II) complexes with tridentate aminoether or aminoalcohol ligands, Polyhedron. 175 (2020) 114228. https://doi.org/10.1016/j.poly.2019.114228.
[58] T.A. Fernandes, M. V Kirillova, V. André, A.M. Kirillov, Interplay between H-bonding and interpenetration in an aqueous copper(II)–aminoalcohol–pyromellitic acid system: self-assembly synthesis, structural features and catalysis, Dalton Trans. 47 (2018) 16674–16683.

https://doi.org/10.1039/C8DT02983K.
[59] F. Sama, A.K. Dhara, M.N. Akhtar, Y.-C. Chen, M.-L. Tong, I.A. Ansari, M. Raizada, M. Ahmad, M. Shahid, Z.A. Siddiqi, Aminoalcohols and benzoates-friends or foes? Tuning nuclearity of Cu(II) complexes, studies of their structures, magnetism, and catecholase-like activities as well as performing DFT and TDDFT studies, Dalton Trans. 46 (2017) 9801–9823. https://doi.org/10.1039/C7DT01571B.
[60] E.A. Buvaylo, V.N. Kokozay, O.Y. Vassilyeva, B.W. Skelton, J. Jezierska, Cu/Cd heterometallic solids with the [Cu(Hdea)(H2dea)]22+ motif (H2dea=diethanolamine): Exchange interactions through hydrogen bonding, Inorg. Chim. Acta. 362 (2009) 2429–2434. https://doi.org/10.1016/j.ica.2008.10.037.
[61] J. Zhang, L.G. Hubert-Pfalzgraf, D. Luneau, Interplay between aminoalcohols and trifluoroacetate ligands: Ba–Cu heterometallics or cocrystallization of homometallics?, Inorg. Chem. Commun. 7 (2004) 979–984. https://doi.org/10.1016/j.inoche.2004.06.012.
[62] V.A. Potaskalov, N.I. Potaskalova, I. V Lisokvskaya, T. V Patskova, Structure of an intracomplex compound of Cobalt (III) with triethanolamine, Ukr. Chem. J. 70 (2004) 88–90.
[63] T. Wombacher, R. Goddard, C.W. Lehmann, J.J. Schneider, Bowl shaped deformation in a planar aromatic polycycle upon reduction. Li and Na separated dianions of the aromatic polycycle 5,6:11,12-di-o-phenylene-tetracene, Dalton Trans. 46 (2017) 14122–14129. https://doi.org/10.1039/C7DT03039H.
[64] A.Y. Rogachev, M. Alkan, J. Li, S. Liu, S.N. Spisak, A.S. Filatov, M.A. Petrukhina, Mono-reduced Corannulene: To Couple and Not to Couple in One Crystal, Chem. Eur. J. 25 (2019) 14140–14147. https://doi.org/10.1002/chem.201902992.
[65] J. Luo, Y. Bi, L. Zhang, X. Zhang, T.L. Liu, A Stable, Non-Corrosive Perfluorinated Pinacolatoborate Mg Electrolyte for Rechargeable Mg Batteries, Angew. Chem. Int. Ed. 58 (2019) 6967–6971. https://doi.org/10.1002/anie.201902009.
[66] O. Tutusaus, R. Mohtadi, T.S. Arthur, F. Mizuno, E.G. Nelson, Y. V Sevryugina, An Efficient Halogen-Free Electrolyte for Use in Rechargeable Magnesium Batteries, Angew. Chem. Int. Ed. 54 (2015) 7900–7904. https://doi.org/10.1002/anie.201412202.
[67] F.J. Craig, A.R. Kennedy, R.E. Mulvey, M.D. Spicer, Structures of the potassium aluminate [{K2(Me3AlOBut)2·pmdeta}∞] and [{K(pmdeta)2}+(AlMe4)–]: how the nature of the alane reagent determines which of these products form from alkoxide-containing reaction mixtures, Chem. Commun. (1996) 1951–1952. https://doi.org/10.1039/CC9960001951.
[68] P. van Leeuwen, P. Kamer, J. Reek, The bite angle makes the catalyst, Pure Appl. Chem. 71 (1999) 1443–1452. https://doi.org/10.1351/pac199971081443.
[69] M. Bazargan, M. Mirzaei, A. Franconetti, A. Frontera, On the preferences of five-membered chelate rings in coordination chemistry: insights from the Cambridge Structural Database and theoretical calculations, Dalton Trans. 48 (2019) 5476–5490. https://doi.org/10.1039/C9DT00542K.
[70] A. V Davis, T.K. Firman, B.P. Hay, K.N. Raymond, d-Orbital Effects on Stereochemical Non-Rigidity: Twisted TiIV Intramolecular Dynamics, J. Am. Chem. Soc. 128 (2006) 9484–9496. https://doi.org/10.1021/ja0617946.
[71] S. Merkel, D. Stern, J. Henn, D. Stalke, Solvent-Separated and Contact Ion Pairs of Parent Lithium Trimethyl Zincate, Angew. Chem. Int. Ed. 48 (2009) 6350–6353. https://doi.org/10.1002/anie.200901587.
[72] L.E. Lemmerz, R. McLellan, N.R. Judge, A.R. Kennedy, S.A. Orr, M. Uzelac, E. Hevia, S.D. Robertson, J. Okuda, R.E. Mulvey, Donor-influenced Structure–Activity Correlations in Stoichiometric and Catalytic Reactions of Lithium Monoamido-Monohydrido-Dialkylaluminates, Chem. Eur. J. 24 (2018) 9940–9948. https://doi.org/10.1002/chem.201801541.
[73] W. Schmitt, P.A. Jordan, R.K. Henderson, G.R. Moore, C.E. Anson, A.K. Powell, Synthesis, structures and properties of hydrolytic Al(III) aggregates and Fe(III) analogues formed with

iminodiacetate-based chelating ligands, Coord. Chem. Rev. 228 (2002) 115–126. https://doi.org/10.1016/S0010-8545(02)00110-8.
[74] P.M. Forster, A.K. Cheetham, The role of reaction conditions and ligand flexibility in metal-organic hybrid materials—examples from metal diglycolates and iminodiacetates, Microporous Mesoporous Mater. 73 (2004) 57–64. https://doi.org/10.1016/j.micromeso.2004.02.020.
[75] P. Cancino, L. Santibañez, C. Stevens, P. Fuentealba, N. Audebrand, D. Aravena, J. Torres, S. Martinez, C. Kremer, E. Spodine, Influence of the channel size of isostructural 3d–4f MOFs on the catalytic aerobic oxidation of cycloalkenes, New J. Chem. 43 (2019) 11057–11064. https://doi.org/10.1039/C9NJ02091H.
[76] R. Puentes, J. Torres, C. Kremer, J. Cano, F. Lloret, D. Capucci, A. Bacchi, Mononuclear and polynuclear complexes ligated by an iminodiacetic acid derivative: synthesis, structure, solution studies and magnetic properties, Dalton Trans. 45 (2016) 5356–5373. https://doi.org/10.1039/C5DT05060J.
[77] I. Yousuf, M. Zeeshan, F. Arjmand, M.A. Rizvi, S. Tabassum, Synthesis, structural investigations and DNA cleavage properties of a new water soluble Cu(II)–iminodiacetate complex, Inorg. Chem. Commun. 106 (2019) 48–53. https://doi.org/10.1016/j.inoche.2019.05.027.
[78] M. Sekizaki, Bis(iminodiacetamide)nickel(II) Perchlorate, Acta Cryst. B32 (1976) 1568–1570. https://doi.org/10.1107/S0567740876005839.
[79] N. Smrečki, O. Jović, K. Molčanov, B.-M. Kukovec, I. Kekez, D. Matković-Čalogović, Z. Popović, Influence of the non-coordinating alkyl chain type in N-alkylated iminodiacetamides on the stability and structure of their complexes with nickel(II) and cobalt(II), Polyhedron. 130 (2017) 115–126. https://doi.org/10.1016/j.poly.2017.03.060.
[80] N. Smrečki, O. Jović, B.-M. Kukovec, E. Šimunić, S. Vuk, A. Skuhala, M. Babić, T. Rončević, N. Ilić, I. Kekez, D. Matković-Čalogović, Z. Popović, Copper(II) complexes with N-alkyliminodiacetamide ligands. Preparation, structural, spectroscopic and DFT studies and biological evaluation, Inorg. Chim. Acta. 471 (2018) 521–529. https://doi.org/10.1016/j.ica.2017.11.038.
[81] Y. Mikata, Y. Sato, S. Takeuchi, Y. Kuroda, H. Konno, S. Iwatsuki, Quinoline-based fluorescent zinc sensors with enhanced fluorescence intensity, Zn/Cd selectivity and metal binding affinity by conformational restriction., Dalton Trans. 42 (2013) 9688–9698. https://doi.org/10.1039/c3dt50719j.
[82] A. Malassa, C. Agthe, H. Görls, M. Friedrich, M. Westerhausen, Deprotonation and dehydrogenation of Di(2-pyridylmethyl)amine with M[N(SiMe3)2]2 (M = Mn, Fe, Co, Zn) and Fe(C6H2-2,4,6-Me3)2, J. Organomet. Chem. 695 (2010) 1641–1650. https://doi.org/10.1016/j.jorganchem.2010.04.009.
[83] B.A. Frazier, P.T. Wolczanski, E.B. Lobkovsky, T.R. Cundari, Unusual Electronic Features and Reactivity of the Dipyridylazaallyl Ligand: Characterizations of (smif)2M [M = Fe, Co, Co+, Ni; smif = {(2-py)CH}2N] and [(TMS)2NFe]2(smif)2, J. Am. Chem. Soc. 131 (2009) 3428–3429. https://doi.org/10.1021/ja8089747.
[84] K. Seubert, D. Böhme, J. Kösters, W.-Z. Shen, E. Freisinger, J. Müller, N-Methyl-2, 2'-Dipicolylamine Complexes as Potential Models for Metal-Mediated Base Pairs, Z. Anorg. Allg. Chem. 638 (2012) 1761–1767. https://doi.org/10.1002/zaac.201200089.
[85] G.H. Eom, J.H. Kim, Y.D. Jo, E.Y. Kim, J.M. Bae, C. Kim, S.-J. Kim, Y. Kim, Anion effects on construction of cadmium(II) compounds with a chelating ligand bis(2-pyridylmethyl)amine: Their photoluminescence and catalytic activities, Inorg. Chim. Acta. 387 (2012) 106–116. https://doi.org/10.1016/j.ica.2012.01.002.
[86] R. Diaz-Torres, S. Alvarez, Coordinating ability of anions and solvents towards transition metals and lanthanides, Dalton Trans. 40 (2011) 10742–10750. https://doi.org/10.1039/c1dt11184a.
[87] R. Bala, A. Kaur, G. Amalija, One-pot synthetic approach to isolate a single isomer of

bis(diethylenetriamine)cobalt(III) cation in bulk using benzoates and the isomeric effects of the cation on ion association with anions, J. Coord. Chem. 69 (2016) 1–25. https://doi.org/10.1080/00958972.2016.1159303.
[88] S.J. Pike, J.J. Hutchinson, C.A. Hunter, H-Bond Acceptor Parameters for Anions, J. Am. Chem. Soc. 139 (2017) 6700–6706. https://doi.org/10.1021/jacs.7b02008.
[89] Đ. Škalamera, E. Sanders, R. Vianello, A. Maršavelski, A. Pevec, I. Turel, S.I. Kirin, Synthesis and characterization of ML and ML2 metal complexes with amino acid substituted bis(2-picolyl)amine ligands, Dalton Trans. 45 (2016) 2845–2858. https://doi.org/10.1039/C5DT03387J.
[90] N. Pantalon Juraj, S. Muratović, B. Perić, N. Šijaković Vujičić, R. Vianello, D. Žilić, Z. Jagličić, S.I. Kirin, Stuctural Variety of Isopropyl-bis(2-picolyl)amine Complexes with Zinc(II) and Copper(II), Cryst. Growth Des. 20 (2020) 2440–2453. https://doi.org/10.1021/acs.cgd.9b01625.
[91] H. Wu, Z. Yang, F. Wang, H. Peng, H. Zhang, C. Wang, K. Wang, V-shaped ligand 1,3-bis(1-ethylbenzimidazol-2-yl)-2-thiapropane and manganese(II), cobalt(II) and copper(II) complexes: Synthesis, crystal structure, DNA-binding properties and antioxidant activities, J. Photochem. Photobiol. B Biol. 148 (2015) 252–261. https://doi.org/10.1016/j.jphotobiol.2015.04.014.
[92] F. Weisser, H. Stevens, J. Klein, M. van der Meer, S. Hohloch, B. Sarkar, Tailoring RuII Pyridine/Triazole Oxygenation Catalysts and Using Photoreactivity to Probe their Electronic Properties, Chem. Eur. J. 21 (2015) 8926–8938. https://doi.org/10.1002/chem.201406441.
[93] D. Schweinfurth, L. Hettmanczyk, L. Suntrup, B. Sarkar, Metal Complexes of Click-Derived Triazoles and Mesoionic Carbenes: Electron Transfer, Photochemistry, Magnetic Bistability, and Catalysis, Z. Anorg. Allg. Chem. 643 (2017) 554–584. https://doi.org/10.1002/zaac.201700030.
[94] D. Schweinfurth, F. Weisser, D. Bubrin, L. Bogani, B. Sarkar, Cobalt Complexes with “Click”-Derived Functional Tripodal Ligands: Spin Crossover and Coordination Ambivalence, Inorg. Chem. 50 (2011) 6114–6121. https://doi.org/10.1021/ic200246v.
[95] N. Pantalon Juraj, M. Krklec, T. Novosel, B. Perić, R. Vianello, S. Raić-Malić, S.I. Kirin, Copper(II) and zinc(II) complexes of mono- and bis-1,2,3-triazole-substituted heterocyclic ligands, Dalton Trans. 49 (2020) 9002–9015. https://doi.org/10.1039/D0DT01244K.
[96] T.K. Paine, T. Weyhermüller, L.D. Slep, F. Neese, E. Bill, E. Bothe, K. Wieghardt, P. Chaudhuri, Nonoxovanadium(IV) and Oxovanadium(V) Complexes with Mixed O, X, O-Donor Ligands (X = S, Se, P, or PO), Inorg. Chem. 43 (2004) 7324–7338. https://doi.org/10.1021/ic040052f.
[97] F. Thomas, G. Gellon, I. Gautier-Luneau, E. Saint-Aman, J.-L. Pierre, A structural and functional model of galactose oxidase: control of the one-electron oxidized active form through two differentiated phenolic arms in a tripodal ligand., Angew. Chem. Int. Ed. Engl. 41 (2002) 3047–3050. https://doi.org/10.1002/1521-3773(20020816)41:16<3047::AID-ANIE3047>3.0.CO;2-W.
[98] L. Duan, Y.-B. Jia, X.-G. Li, Y.-M. Li, H. Hu, J. Li, C. Cui, Synthesis, Characterization, and Reversible Multielectron Redox Properties of a Biradical Yttrium Complex Containing Bis(2-isopropylaminophenyl)amide, Eur. J. Inorg. Chem. 2017 (2017) 2231–2235. https://doi.org/10.1002/ejic.201601457.
[99] R. Sikari, S. Sinha, U. Jash, S. Das, P. Brandão, B. de Bruin, N.D. Paul, Deprotonation Induced Ligand Oxidation in a NiII Complex of a Redox Noninnocent N1-(2-Aminophenyl)benzene-1,2-diamine and Its Use in Catalytic Alcohol Oxidation, Inorg. Chem. 55 (2016) 6114–6123. https://doi.org/10.1021/acs.inorgchem.6b00646.
[100] M.K. Wojnar, J.W. Ziller, A.F. Heyduk, Heterobimetallic and Heterotrimetallic Clusters Containing a Redox-Active Metalloligand, Eur. J. Inorg. Chem. 2017 (2017) 5571–5575. https://doi.org/10.1002/ejic.201701222.
[101] C.-K. Chiang, K.-T. Chu, C.-C. Lin, S.-R. Xie, Y.-C. Liu, S. Demeshko, G.-H. Lee, F. Meyer, M.-L.

Tsai, M.-H. Chiang, C.-M. Lee, Photoinduced NO and HNO Production from Mononuclear {FeNO}6 Complex Bearing a Pendant Thiol, J. Am. Chem. Soc. 142 (2020) 8649–8661. https://doi.org/10.1021/jacs.9b13837.
[102] S. Shekar, S.N. Brown, Migrations of Alkyl and Aryl Groups from Silicon to Nitrogen in Silylated Aryloxyiminoquinones, Organometallics. 32 (2013) 556–564. https://doi.org/10.1021/om301028c.
[103] M. Mijanuddin, A.D. Jana, A. Ray, M.G.B. Drew, K.K. Das, A. Pramanik, M. Ali, Geometrical isomers of [TEAH][Co(LSe)2]·xH2O: synthesis, structural, spectroscopic and computational studies, Dalton Trans. (2009) 5164–5170. https://doi.org/10.1039/B901040H.
[104] Y.-Y. Wu, J.-C. Hong, R.-F. Tsai, H.-R. Pan, B.-H. Huang, Y.-W. Chiang, G.-H. Lee, M.-J. Cheng, H.-F. Hsu, Ligand-Based Reactivity of Oxygenation and Alkylation in Cobalt Complexes Binding with (Thiolato)phosphine Derivatives, Inorg. Chem. 59 (2020) 4650–4660. https://doi.org/10.1021/acs.inorgchem.9b03740.
[105] H.-C. Chang, S.-H. Lin, Y.-C. Hsu, S.-W. Jen, W.-Z. Lee, Nickel(III)-mediated oxidative cascades from a thiol-bearing nickel(II) precursor to the nickel(IV) product, Dalton Trans. 47 (2018) 3796–3802. https://doi.org/10.1039/C7DT04137C.
[106] Y. Li, A. Turnas, J.T. Ciszewski, A.L. Odom, Group-4 η1-Pyrrolyl Complexes Incorporating N,N-Di(pyrrolyl-α-methyl)-N-methylamine, Inorg. Chem. 41 (2002) 6298–6306. https://doi.org/10.1021/ic0259484.
[107] A. Adach, M. Daszkiewicz, M. Duczmal, Z. Staszak, Cobalt(II) complex containing two-ring scorpionate-like ligands formed in situ. Studies on the [Co0–1-hydroxymethyl-3,5-dimethylpyrazole–MoO3–NH4I] system, Inorg. Chem. Commun. 35 (2013) 22–26. https://doi.org/10.1016/j.inoche.2013.05.001.
[108] C.-C. Du, J.-Z. Fan, X.-F. Wang, S.-B. Zhou, D.-Z. Wang, New metal-organic complexes based on bis(tetrazole) ligands: Synthesis, structures and properties, J. Mol. Struct. 1133 (2017) 348–357. https://doi.org/10.1016/j.molstruc.2016.12.033.
[109] A. Kermagoret, F. Tomicki, P. Braunstein, Nickel and iron complexes with N,P,N-type ligands: synthesis, structure and catalytic oligomerization of ethylene, Dalton Trans. (2008) 2945–2955. https://doi.org/10.1039/B802009D.
[110] C.J. Whiteoak, J.D. Nobbs, E. Kiryushchenkov, S. Pagano, A.J.P. White, G.J.P. Britovsek, Tri(pyridylmethyl)phosphine: The Elusive Congener of TPA Shows Surprisingly Different Coordination Behavior, Inorg. Chem. 52 (2013) 7000–7009. https://doi.org/10.1021/ic4005196.
[111] V. Brune, C. Hegemann, S. Mathur, Molecular Routes to Two-Dimensional Metal Dichalcogenides MX2 (M = Mo, W; X = S, Se), Inorg. Chem. 58 (2019) 9922–9934. https://doi.org/10.1021/acs.inorgchem.9b01084.
[112] Y.D. Boyko, A.Y. Sukhorukov, A.N. Semakin, Y. V Nelyubina, I. V Ananyev, K.S. Rangappa, S.L. Ioffe, Synthesis, structure and dioxygen reactivity of Ni(II) complexes with mono-, bis-, tetra- and hexa-oxime ligands, Polyhedron. 71 (2014) 24–33. https://doi.org/10.1016/j.poly.2014.01.003.
[113] K. Gholivand, A. Reza Farrokhi, Supramolecular Hydrogen-Bonded Frameworks from a New Bisphosphonic Acid and Transition Metal Ions, Z. Anorg. Allg. Chem. 637 (2011) 263–268. https://doi.org/10.1002/zaac.201000280.
[114] M. Garcìa-Basallote, P. Valerga, M.C. Puerta-Vizcaíno, A. Romero, A. Vegas, M. Martínez-Ripoll, An unexpected molybdenum(0) complex with “MoP6” coordination: crystal structure of [Mo{P(CH2CH2PPh2)3}2] · C5H10, J. Organomet. Chem. 420 (1991) 371–377. https://doi.org/10.1016/0022-328X(91)86465-3.
[115] B. Glowacki, R. Pallach, M. Lutter, F. Roesler, H. Alnasr, C. Thomas, D. Schollmeyer, K. Jurkschat, Cis versus Trans: The Coordination Environment about the Tin(IV) Atom in Spirocyclic Amino Alcohol Derivatives, Chem. Eur. J. 24 (2018) 19266–19279. https://doi.org/10.1002/chem.201803952.

[116] K. Uemura, R. Miyake, Paramagnetic One-Dimensional Chain Complex Consisting of Three Kinds of Metallic Species Showing Magnetic Interaction through Metal–Metal Bonds, Inorg. Chem. 59 (2020) 1692–1701. https://doi.org/10.1021/acs.inorgchem.9b02844.
[117] K. Uemura, M. Ebihara, Paramagnetic One-Dimensional Chains Comprised of Trinuclear Pt–Cu–Pt and Paddlewheel Dirhodium Complexes with Metal–Metal Bonds, Inorg. Chem. 52 (2013) 5535–5550. https://doi.org/10.1021/ic400470g.
[118] W. Chen, K. Matsumoto, Synthesis and Structural Characterization of Trinuclear, Amidate-Bridged Heterobimetallic Complexes [{Pt(NH3)2(NHCOtBu)2}2M]Xn (M = Mn, Fe, Co, Ni, Cu; X = BF4−, ClO4−; n = 2 or 3), Eur. J. Inorg. Chem. 2002 (2002) 2664–2670. https://doi.org/10.1002/1099-0682(200210)2002:10<2664::AID-EJIC2664>3.0.CO;2-T.
[119] H.H. Murray, D.A. Briggs, G. Garzon, R.G. Raptis, L.C. Porter, J.P. Fackler, Structural characterization of a linear [Au.cntdot..cntdot..cntdot.Pt.cntdot..cntdot..cntdot.Au] complex, Au2Pt(CH2P(S)Ph2)4, and its oxidized linear metal-metal bonded [Au-Pt-Au] product, Au2Pt(CH2P(S)Ph2)4Cl2, Organometallics. 6 (1987) 1992–1995. https://doi.org/10.1021/om00152a030.
[120] H. Schmidbaur, C. Hartmann, G. Reber, G. Müller, Isovalent and Mixed-Valent Ylide Complexes of Gold: The Synthesis of Trinuclear Compounds Having Double Paddlewheel Structure, Angew. Chem. Int. Ed. English. 26 (1987) 1146–1148. https://doi.org/10.1002/anie.198711461.
[121] C. King, D.D. Heinrich, J.C. Wang, J.P. Fackler, G. Garzon, Symmetric addition of sulfur dioxide to linear bi- and trinuclear gold(I) compounds. Partial oxidation to form [Au(.mu.-(CH2)2PPh2)]2(SO2)2 and Au2Pt(.mu.-C,S-CH2PPh2S)4(SO2)2, J. Am. Chem. Soc. 111 (1989) 2300–2302. https://doi.org/10.1021/ja00188a053.
[122] R.G. Pearson, Hard and Soft Acids and Bases, J. Am. Chem. Soc. 85 (1963) 3533–3539. https://doi.org/10.1021/ja00905a001.
[123] C. Förster, T.E. Gorelik, U. Kolb, V. Ksenofontov, K. Heinze, Crystalline Non-Equilibrium Phase of a Cobalt(II) Complex with Tridentate Ligands, Eur. J. Inorg. Chem. 2015 (2015) 920–924. https://doi.org/10.1002/ejic.201403200.
[124] A. Tatehata, S. Yamada, A. Muraida, Isomer Distribution and Stereoselectivity in Electron Transfer Reactions of [Co(dien)2]2+ with Anionic Cobalt(III) Complexes, Bull. Chem. Soc. Jpn. 73 (2000) 1135–1142. https://doi.org/10.1246/bcsj.73.1135.
[125] S.E. Howson, N.P. Chmel, G.J. Clarkson, R.J. Deeth, D.H. Simpson, P. Scott, Jahn–Teller effects on π-stacking and stereoselectivity in the phenylethaniminopyridine tris-chelates Cu(NN')32+, Dalton Trans. 41 (2012) 4477–4483. https://doi.org/10.1039/C2DT12378A.
[126] M. Melník, Structural isomerism of copper(II) compounds, Coord. Chem. Rev. 47 (1982) 239–261. https://doi.org/10.1016/0010-8545(82)85033-9.
[127] L.R. Gahan, T.W. Hambley, G.H. Searle, M.J. Bjerrum, E. Larsen, The isomers of the bis(1-thia-4,7-diazacyclononane)cobalt(III) ion: separation and characterization, Inorg. Chim. Acta. 147 (1988) 17–26. https://doi.org/10.1016/S0020-1693(00)80624-6.
[128] J.C.A. Boeyens, S.M. Dobson, R.D. Hancock, Structures of bis(1-thia-4,7-diazacyclononane)copper(II) nitrate and bis(1,7-diaza-4-thiaheptane)copper(II) nitrate. A different conformation for the coordinated macrocycle, Inorg. Chem. 24 (1985) 3073–3076. https://doi.org/10.1021/ic00213a041.
[129] J. Echeverría, E. Cremades, A.J. Amoroso, S. Alvarez, Jahn–Teller distortions of six-coordinate CuII compounds: cis or trans?, Chem. Commun. (2009) 4242–4244. https://doi.org/10.1039/B903867A.
[130] G. Searle, E. Larsen, The Bis[di(2-aminoethyl)sulfide]cobalt(III) Ion. Existence of only the Unsymmetrical-facial Geometric Isomer and Its Optical Resolution, Acta Chem. Scand. 30a (1976) 143–151. https://doi.org/10.3891/acta.chem.scand.30a-0143.
[131] C.J. Carrano, B.S. Chohan, B.S. Hammes, B.W. Kail, V.N. Nemykin, P. Basu, Donor Atom Dependent Geometric Isomers in Mononuclear Oxo−Molybdenum(V) Complexes:

Implications for Coordinated Endogenous Ligation in Molybdoenzymes, Inorg. Chem. 42 (2003) 5999–6007. https://doi.org/10.1021/ic0262785.
[132] R.G. Pearson, Hard and soft acids and bases—the evolution of a chemical concept, Coord. Chem. Rev. 100 (1990) 403–425. https://doi.org/10.1016/0010-8545(90)85016-L.
[133] M. Zafar, R. Rongala, A.N. Pradhan, K. Pathak, T. Roisnel, J.-F. Halet, S. Ghosh, Mercapto-benzothiazolyl based ruthenium(ii) borate complexes: synthesis and reactivity towards various phosphines, Dalton Trans. 48 (2019) 7413–7424. https://doi.org/10.1039/C9DT00498J.
[134] M.P. Coles, M.S. Khalaf, P.B. Hitchcock, A new aliphatic N,C,N'-pincer ligand with pendant guanidine groups, Inorg. Chim. Acta. 422 (2014) 228–234. https://doi.org/10.1016/j.ica.2014.05.021.
[135] S. Azpeitia, B. Fernández, M.A. Garralda, M.A. Huertos, Dehydrogenative Coupling of a Tertiary Silane Using Wilkinson's Catalyst, Eur. J. Inorg. Chem. 2016 (2016) 2891–2895. https://doi.org/10.1002/ejic.201600395.
[136] A.F. Hill, H. Neumann, J. Wagler, Bis(methimazolyl)silyl Complexes of Ruthenium, Organometallics. 29 (2010) 1026–1031. https://doi.org/10.1021/om901067t.
[137] R. Hoffmann, J.M. Howell, A.R. Rossi, Bicapped tetrahedral, trigonal prismatic, and octahedral alternatives in main and transition group six-coordination, J. Am. Chem. Soc. 98 (1976) 2484–2492. https://doi.org/10.1021/ja00425a016.
[138] T. Pandiyan, J.G. Hernández, N.T. Medina, S. Bernés, Geometrical isomers of bis(benzimidazol-2-ylethyl)sulfide)cobalt(II) diperchlorates: synthesis, structure, spectra and redox behavior of pink-[Co(bbes)2](ClO4)2 and blue-[Co(bbes)2](ClO4)2, Inorg. Chim. Acta. 357 (2004) 2570–2578. https://doi.org/10.1016/j.ica.2004.02.014.
[139] J. Bjernemose, A. Hazell, C.J. McKenzie, M.F. Mahon, L.P. Nielsen, P.R. Raithby, O. Simonsen, H. Toftlund, J.A. Wolny, Synthesis and characterization of ruthenium(II) complexes with polypicolylamine ligands, Polyhedron. 22 (2003) 875–885. https://doi.org/10.1016/S0277-5387(03)00025-1.
[140] A. Grirrane, A. Pastor, E. Alvarez, C. Mealli, A. Ienco, P. Rosa, A. Galindo, Thiodiacetate and Oxydiacetate Cobalt Complexes: Synthesis, Structure and Stereochemical Features, Eur. J. Inorg. Chem. 2007 (2007) 3543–3552. https://doi.org/10.1002/ejic.200700075.
[141] A. Hammershoi, E. Larsen, S. Larsen, E. Näsäkkälä, O. Bastiansen, L. Fernholt, G. Gundersen, C. Nielsen, B. Cyvin, S. Cyvin, The Crystal Structure of (---)D-u-fac-Bis[di(2-aminoethyl)sulfide]cobalt(III) Chloride Dihydrate and the Absolute Configuration of the Cation, Acta Chem. Scand. 32a (1978) 501–507. https://doi.org/10.3891/acta.chem.scand.32a-0501.
[142] P. Li, B. de Bruin, J.N.H. Reek, W.I. Dzik, Photo- and Thermal Isomerization of (TP)Fe(CO)Cl2 [TP = Bis(2-diphenylphosphinophenyl)phenylphosphine], Organometallics. 34 (2015) 5009–5014. https://doi.org/10.1021/acs.organomet.5b00644.
[143] G.H. Searle, M. Petkovic, F.R. Keene, Cobalt(III) complexes of 4,7-dimethyl-1,4,7,10-tetraazadecane. Preparations, stereochemistry, and reactions, and the effect of N-methyllation on relative isomer stabilities, Inorg. Chem. 13 (1974) 399–408. https://doi.org/10.1021/ic50132a033.
[144] K. V Zaitsev, S.S. Karlov, A.A. Selina, Y.F. Oprunenko, A. V Churakov, B. Neumüller, J.A.K. Howard, G.S. Zaitseva, Titanium Complexes of Dialkanolamine Ligands: Synthesis and Structure, Eur. J. Inorg. Chem. 2006 (2006) 1987–1999. https://doi.org/10.1002/ejic.200501154.
[145] H. Follner, Die Kristallstruktur von Sn[(OC2H4)2NC2H4OH]2, Monatsh. Chem. 103 (1972) 1438–1443. https://doi.org/10.1007/BF00904527.
[146] T. Zöller, L. Iovkova-Berends, C. Dietz, T. Berends, K. Jurkschat, On the Reaction of Elemental Tin with Alcohols: A Straightforward Approach to Tin(II) and Tin(IV) Alkoxides and Related Tinoxo Clusters, Chem. Eur. J. 17 (2011) 2361–2364.

https://doi.org/10.1002/chem.201003338.
[147] T. Kemmitt, N.I. Al-Salim, G.J. Gainsford, W. Henderson, Titanium Amino Alcohol Complexes from α-Titanic Acid: X-Ray Crystal Structure of Titanium Bis[2,2'-(methylimino)diethanolate], Aust. J. Chem. 52 (1999) 915–920. https://doi.org/10.1071/CH99089.
[148] Y. Kushi, T. Ideno, T. Yasui, H. Yoneda, The Crystal and Molecular Structure of Potassium u-fac-Bis(N-methyliminodiacetato)cobaltate(III) Sesquihydrate, Bull. Chem. Soc. Jpn. 56 (1983) 2845–2846. https://doi.org/10.1246/bcsj.56.2845.
[149] Y. Yamasaki, T. Kurisaki, T. Yamaguchi, H. Wakita, Determination of the absolute configuration of sodium (-)589-bis-N-methyliminodiacetato)cobaltate(III) trihydate, Acta Cryst. C49 (1993) 229–231. https://doi.org/10.1107/S0108270192006401.
[150] J. Tu, H. Chen, H. Tian, X. Yu, B. Zheng, S. Zhang, P. Ma, Temperature-induced structural transformations accompanied by changes in magnetic properties of two copper coordination polymers, CrystEngComm. 22 (2020) 3482–3488. https://doi.org/10.1039/D0CE00391C.
[151] G.H. Searle, F.R. Keene, S.F. Lincoln, Homogeneous and charcoal-catalyzed isomerizations of the (diethylenetriamine)(methyldiethylenetriamine)cobalt(III) and bis(diethylenetriamine)cobalt(III) ions, Inorg. Chem. 17 (1978) 2362–2369. https://doi.org/10.1021/ic50187a006.
[152] H. Kawaguchi, T. Ama, T. Yasui, The Base-Catalyzed Isomerization of the (Iminodiacetato)-(N-methyliminodiacetato)cobaltate(III) and Bis(iminodiacetato)cobaltate(III) Ions, Bull. Chem. Soc. Jpn. 57 (1984) 2422–2427. https://doi.org/10.1246/bcsj.57.2422.
[153] B. Maity, S. Gadadhar, T.K. Goswami, A.A. Karande, A.R. Chakravarty, Impact of metal on the DNA photocleavage activity and cytotoxicity of ferrocenyl terpyridine 3d metal complexes, Dalton Trans. 40 (2011) 11904–11913. https://doi.org/10.1039/C1DT11102G.
[154] J. Glerup, P.A. Goodson, D.J. Hodgson, K. Michelsen, K.M. Nielsen, H. Weihe, Synthesis and Characterization of Bis(2-pyridylmethyl)amine Complexes of Manganese(II), Zinc(II), and Cadmium (II), Inorg. Chem. 31 (1992) 4611–4616. https://doi.org/10.1021/ic00048a032.
[155] R. Stähler, W. Bensch, Solvothermal Synthesis and Crystal Structure of the New Layered Thioantimonate(III) [Ni(C4H13N3)2]9Sb22S42 · 0.5H2O: Interconnection of the SbS3, SbS4, and SbS5 Primary Building Units Yielding the Very Large Sb30S30 Heteroring, Z. Anorg. Allg. Chem. 628 (2002) 1657–1662. https://doi.org/10.1002/1521-3749(200207)628:7<1657::AID-ZAAC1657>3.0.CO;2-C.
[156] T.G. Appleton, Donor atom preferences in complexes of platinum and palladium with amino acids and related molecules, Coord. Chem. Rev. 166 (1997) 313–359. https://doi.org/10.1016/S0010-8545(97)00047-7.
[157] A.K. Mukherjee, S. Koner, A. Ghosh, N.R. Chaudhuri, M. Mukherjee, A.J. Welch, Isomerism in bis(diethylenetriamine)nickel(II) thiocyanate: synthesis, solid-state interconversion and X-ray crystallographic study of sym-fac and mer isomers, J. Chem. Soc. Dalton Trans. (1994) 2367–2371. https://doi.org/10.1039/DT9940002367.
[158] K. Sakakibara, Y. Yoshikawa, H. Yamatera, Isomerism of the Metal Complexes Containing Multidentate Ligands. VIII. Chromatographic Behavior of [CoN6]3+-type Complexes on an SP-Sephadex Column, Bull. Chem. Soc. Jpn. 52 (1979) 2725–2726. https://doi.org/10.1246/bcsj.52.2725.